



FUNDAÇÃO EDSON QUEIROZ
UNIVERSIDADE DE FORTALEZA
ENSINANDO E APRENDENDO



UNIVERSITAT POLITÈCNICA
DE CATALUNYA

A CASE STUDY ON THE COMMUNICATIONS SUBSYSTEM FOR CUBESAT

NATALIA CEBRIÁN HERRERA

Trabalho de Conclusão de Curso – TCC a ser
apresentado e submetido à avaliação para
conclusão do Curso de Ciência da Computação
do centro de Ciências Tecnológicas da
Universidade de Fortaleza.

Tutor: Antonio Macilio Pereira de Lucena

ANALYSIS AND IMPROVEMENT OF BRAZILIAN SATELLITE LINK

Natalia Cebrián Herrera

PARECER: _____

Data: 09/06/2014

BANCA EXAMINADORA:

A.Macilio Pereira de Lucena

Clauson Sales do Nascimento Rios

Wellington Alves de Brito

Contents

CHAPTER 1

1.1 Abstract.....	10
1.2 Historical Overview	10
1.2.1 Communications.....	10
1.2.2. Spatial communications	11
1.2.3 Cubesat	12
1.3 Objectives.....	12
1.4 Metodology	12

CHAPTER 2

2.1 Description of a transmission/reception system.....	14
2.2 Modulation's theory	17
2.2.1 Analogue modulation	18
2.2.2 Digital modulation.....	18
2.2.3 QPSK.....	19
2.2.4 GMSK	21
2.2.5 8PSK.....	23
2.3 Codification's theory	25
2.3.1 Channel coding.....	25
2.3.2 Source coding	26
2.3.3 Reed-Solomon codes.....	27
2.3.4 Convolutional codes.....	28

CHAPTER 3

3.1 Nanosatellites	30
3.2 Cubesat.....	32
3.2.1 Cubesat subsystems	33
• Attitude Control Subsystem (ACS).....	34
• Thermal Control Subsystem (TCS).....	34
• Communication Subsystem (CS)	35
• The structural subsystem (SS)	36
• Data handling subsystem (DHS)	36
• Power Subsystem (PCS)	37

CHAPTER 4

4.1 SBCD (Sistema Brasileiro de Coleta de Dados).....	41
4.2 CONASAT Project	44

CHAPTER 5

5.1 Simulation Results	45
5.1.1 Transmitter.....	45
5.1.2 Channel.....	45
5.1.3 Receiver.....	46
5.1.4 QPSK Model.....	46
5.1.5 8PSK Model	50
5.1.5 GMSK Model.....	55
5.1.6 QPSK with convolutional encoding.....	59
5.2 Results discussion	63

CHAPTER 6

6.1 Communication Subsystem proposed.....	65
6.2 Conclusions.....	65
6.3 Future perspectives.....	68
References	71

List of Figures

Figure 1: Basic communication system	14
Figure 2: More detailed structure of telecommunication system	15
Figure 3: Real Bandpass Noise Power Spectral Density	16
Figure 4: Binary (2 level) FSK modulation [2]	19
Figure 5: QPSK Constellation [24]	20
Figure 6: Eye Diagrams for GMSK with BT=0.3 (left), BT=0.5 (centre) and BT=1 (right)	22
Figure 7(a): BT=0.3	21
Figure 7(b): BT=0.5	21
Figure 8: GMSK Modulator	23
Figure 9: Structure of Reed-Solomon Code	27
Figure 10: First Cubesat model [1]	31
Figure 11: Second proposed Cubesat model [1]	31
Figure 12: Actual used Cubesat model [1]	32
Figure 13: Communication Window in terms of AOS and LOS	33
Figure 14: Satellite Cubesat subsystems	34
Figure 15: Space Thermal Environment	35
Figure 16: General Layout of the Cubesat Power Subsystem	37
Figure 17: Power Requirement Breakdown by Subsystem	38
Figure 18: Constellation of Brazilian SCD satellite system [18]	43
Figure 19: QPSK Simulation Model (Transmitter)	47
Figure 20: QPSK Simulation Model (AWGN channel)	48
Figure 21: QPSK Simulation Model (Receiver)	48
Figure 22(a): Signal constellation after Raised Cosine Transmit Filter	48
Figure 22(b): Signal constellation after Raised Cosine Receive Filter	49
Figure 23: Spectrum Analyzer Results	49
Figure 24: BER comparative between QPSK theoretic and the model	50
Figure 25: Spectrum Analyzer Results	51
Figure 26(a): Signal constellation after Raised Cosine Transmit Filter	50
Figure 26(b): Signal constellation after Raised Cosine Receive Filter	51
Figure 27: 8-PSK Simulation Model (Transmitter)	52
Figure 28: 8PSK Simulation Model (AWGN Channel)	53
Figure 29: 8PSK Simulation Model (Receiver)	54
Figure 30: 8-PSK Ber comparative	55
Figure 31: Spectrum Analyzer results	56
Figure 32: GMSK Simulation Model (Transmitter)	56
Figure 33: GMSK Simulation Model (AWGN channel)	57
Figure 34: GMSK Simulation Model (Receiver)	58
Figure 35: GMSK BER comparative	59
Figure 36: QPSK with convolutional encoding Simulation Model (Transmitter)	60
Figure 37: QPSK with convolutional encoding Simulation Model (Transmitter)	61
Figure 38: QPSK with convolutional encoding Simulation Model (Transmitter)	61
Figure 39: QPSK with convolutional encoding spectrum before AWGN channel	62
Figure 40: QPSK with Convolutional encoding BER comparative	62

Figure 41: BER comparative between the 4 simulation63

List of tables

Table 1: Cubesat requirements	33
Table 2: Minimum Baud Rate Calculation.....	38
Table 3: SCD-1/SCD-2 technic characteristics.....	42
Table 4: CBERS-1/CBERS-2 technic charateristics.....	42
Table 5: Current Conasat communication subsystem specifications	65
Table 6: Conasat communication subsystem proposed specifications.....	68

Acknowledgments

I would like to thank the Universidade de Fortaleza, Fundação Edson Queiroz for giving me the opportunity to start and develop this project in Fortaleza. To Professor Antonio Macilio Lucena Pereira to trust me from the beginning and to give me the chance to work with him. To Professor Genevides because he tried so hard so I could come to Fortaleza to do my Thesis. To Professor Jose Antonio Lázaro for his support in the distance.

I want to thank Universitat Politècnica de Catalunya not only for the technical knowledge I was able to acquire over the years I spent there, but for values such as hard work and endurance, as well as the ability to cope with difficulties no matter what. I never gave up with my wish to study in Brasil because of these values.

I want to thank my friend, travel mate, and sister for life Gabi Margareto, because without her this adventure would never have been the same. She made me feel home away from home, always. To all the people I shared this experience with: housemates (specially Rainá Jan), the spanish group and all the people I met in Fortaleza, all my friends in Spain, who were supporting me and helping me through the good and specially through the hard times. Thanks to Alvaro García, who helped us in the previous months and cheered us up to never give up.

I want to thank specially my family, my dad my mum and my little brother, because I know it was hard for them to let me go, but they respected my decision and gave me all their love and support. They made the distance easier and make me feel the most fortunate girl in the world because I have them in my life.

CHAPTER 1

1.1 Abstract

Due to the overwhelming increment transmission and reception of information around the world, Satellite Communications have become an essential application in our lives. Proof of this, are the continuous investments made by technology companies to develop new and improved communication satellite systems.

This project focuses on the transmission of data, from the different meteorological stations placed all around Brazil, to the Cubesats set in the brazilian satellites (SCD-1, SCD-2 and CBERS). It also studies the reception in the Cubesat, and the transmission of all the information accumulated to the main reception Station in Cuiabá.

The main objective of this simulation evaluation is to determine the Bit-Error-Rate performance of the models with different modulations and convolutional code in a noisy communication channel. M-Ary Phase Shift Keying (M-PSK) and Gaussian Minimum Shift Keying (GMSK) modulation techniques are used for this simulation evaluation of the coded communication system.

For the model based simulation evaluation the MATLAB/SIMULINK is chosen as the investigating tool. Monte Carlo method of simulation is used for plotting the results in between Bit-Error-Rate (BER) and Signal to Noise ratio (E_b/N_o).

1.2 Historical Overview

1.2.1 Communications

Communication is as old-established as humanity. In ancient times drums and smoke were used to transmit information between distant towns. As a matter of time, and with the electricity era, other techniques were established, like the telegraph and its associated code (1834), which we owe to Samuel Morse. That invent was a huge step in the human communication, but had a big handicap: the impossibility of automatic transmission.

In 1880, Alexander Graham Bell and his assistant, Charles Sumner Tainter, created

the Photophone, at Bell's newly established Volta Laboratory in Washington DC. The device allowed for the transmission of sound on a beam of light. June 1880, Bell conducted the world's first wireless telephone transmission between two buildings, some 213 meters apart. Its first practical use came in military communication systems many decades later, first for optical telegraphy.

1910 Howard Krum introduced some improvements in the synchronization concept of telegraph and added it to the constant longitude Baudot code. That improvement induced the quick diffusion of telegraph equipment. Baudot's original code was adapted to be sent from a manual keyboard, and no teleprinter equipment was ever constructed that used it in its original form. A major technological step was to replace the Morse code by modulating optical waves in speech transmission.

Around 1920, the main telecommunication basis were established, message commutation and line control. Systems were built over voice communication and character transmissions.

After the Second World War began the commercial development of computer systems. To allow communications between machines and create a network, the only system available was the telephonic service, that was very useful because it had a wide hedge. As the systems were sophisticated, in the beginning of the 50's, some data communication protocols were implemented. At the same time, when the digital signals came out, some changes had to be applied, since the telephonic network isn't a suitable way to transmit digital signals. That's because it has a maximum frequency, so the binary signals are distorted. The changes consisted in generate changes in a fixed frequency signal, called carrier. This operation it's known as modulation. The modem was the device which did the modulation/demodulation operations. The first ones, back in 1979, operated at 300bps. The invention of lasers in the 1960s revolutionized free space optics. Nowadays, we have other devices that do the same thing, with better speed rates, efficiency and power capacity.

1.2.2. Spatial communications

The Space Age was inaugurated by a small satellite - the Sputnik 1- launched by the former Soviet Union on October 4, in 1957. It was a sphere of 58 cm that weighed 83.6 kg. It flew for 22 days at an altitude between 228 and 947km, with no specific function. It was carrying nothing but two radio transmitters of 1 W power, with two long antennas, operating between 20.005 and 40.002 MHz and providing a unique and obstinate - " beep beep beep " - tuned by any radio amateur.

In 1956, before of the launch of Sputnik 1, the U.S. approved the project of the first reconnaissance satellite, Corona (12m resolution) , which would revolutionize intelligence systems since 1960 , replacing the aircraft U-2 spy . One such device, piloted by Francis Gary Powers, CIA officer, was shot down by the USSR and displayed in the parade of May 1 of that year. In 1961, the USSR launched its first

reconnaissance satellite, Zenit (resolution of 10 - 15m).

1.2.3 Cubesat

Cubesat, it's a platform that was created 1999 by Bob Twiggs and Jordi Puig-Suari, in partnership with Stanford University and California Polytechnic State University. The goal was to enable graduate students to be able to design, build, test and operate in space a spacecraft with capabilities similar to that of the first spacecraft, Sputnik. The firsts Cubesats were launched in June 2003, and approximately 75 Cubesats have been placed into orbit as of August 2012.

Therefore, the context of our project offered a great opportunity to design a communication system that takes advantage of all these improvements, and at the same time was realistic and useful for the next years.

1.3 Objectives

The main objectives of this project are listed as follows:

- Presenting the Brazilian environmental data collection system with a constellation of Nano satellites: Conasat Project;
- Propound a change to the service communication subsystem of the satellite from Conasat project;
- Present the Simulink models of downlink modem with their simulation results.

1.4 Metodology

The complexity and the growing needs of the satellite transmission systems makes an inescapably real impact in the time and effort needed for analysis and design. The purpose of any simulation program is the modelling of real devices and following evaluation of benefits. The advantage of using a computer assisted calculation tool lies in the fact that it can serve as a test prior to the physical implementation. This allows the designer or network engineer, not only to know a priori what the limiting variables in each particular case are, but also carry a large number of tests, evaluating the feasibility of a system that would be more costly, both in time and financially, if made on the real system. The proposed tool is based

directly in the MATLAB environment whose characteristics allow calculation and drawing signals at any frequency, indiscriminately to the type of system, the generation, analysis and processing.

The current Simulink software has been used in a wide range of scientific applications including signal processing in real time, telecommunications, wired communications and network design.

CHAPTER 2

2.1 Description of a transmission/reception system

The communication system basically deals with the transmission of information from one point to another using the steps, which are carried out in sequential manner. The system for data transmission makes use of the sender and destination address, and this other so many elements that allows to transfer data from one set of point to another set of point, after dividing the elements of communication system in groups. These interface elements acts as the main component for data communication and all these interface elements are given below.

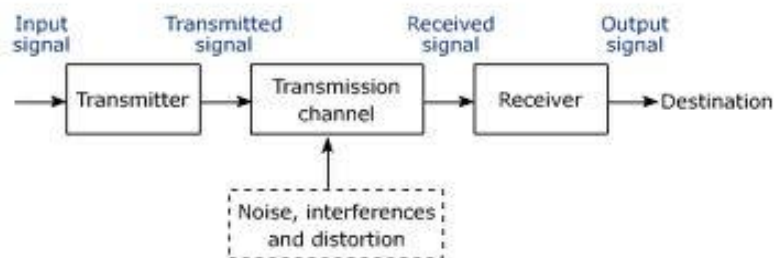


Figure 1: Basic communication system [3]

Each system contains a transmitter. This consists of a source of electrical energy, producing alternating current of a desired frequency of oscillation. The transmitter contains a system to modulate (change) some property of the energy produced to impress a signal on it. The system has to adapt the message to a sequence, in order to send it through the air. In this process the message is adapted to a signal with a fixed frequency called carrier. The carrier is an electric signal with a very higher frequency than the modulator signal. Furthermore, this carrier will be put into another signal, called modulator, which is the one that's going to be sent over the communication channel. This modulation might be as simple as turning the energy on and off, or altering more subtle properties such as amplitude, frequency, phase, or combinations of these properties. The transmitter sends the modulated electrical energy to a tuned resonant antenna; this structure converts the rapidly changing alternating current into an electromagnetic wave that can move through free space (sometimes with a particular polarization).

It's possible to mix some modulations, in order to create a more complex modulation signal. After that, the signal is sent over a channel, which will introduce noise and distortion to the signal. The receiver has to compensate these distortions and noise, and recuperate the original signal with the original information.

A more specific block structure for a typical transmission scenario is illustrated in Figure 2. The source generates a signal s . The source encoder maps the signal s into the bitstream b . The bitstream is transmitted over the error control channel and the received bitstream b' is processed by the source decoder that reconstructs the decoded signal s' and delivers it to the sink. The error characteristic of the digital channel can be controlled by the channel encoder, which adds redundancy to the bits at the source encoder output b . The modulator maps the channel encoder output to an analog signal, which is suitable for transmission over a physical channel. The demodulator interprets the received analog signal as a digital signal, which is fed into the channel decoder. The channel decoder processes the digital signal and produces the received bitstream b' , which may be identical to b even in the presence of channel noise.

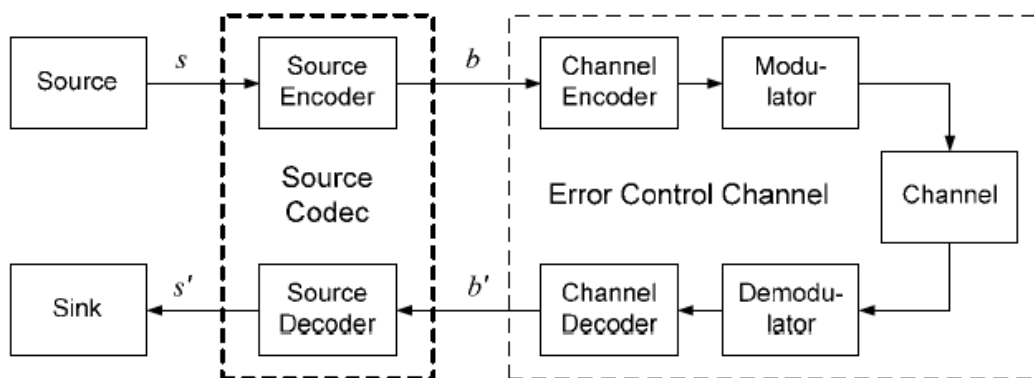


Figure 2: more detailed structure of telecommunication system [3]

The modulation and codification theories are explained in the following chapters.

Due to the degradation of the signal introduced by the channel and the elements in the transmission and reception systems, the delivered signal might not be equal with the sent one. For that reason, it's important to take care of the QoS. The Quality of Service is a set of service requirements to be met by the network while transporting a flow. It's shown in some parameters, which vary depending on the service. The BER, PER, Maximum Delay, Transmission Speed are some of them.

In our case, we are working on the hypothetical case of a channel that introduces an AWGN noise. The Additive white Gaussian noise has been chosen because of its characteristics:

- Additive' because it is added to any noise that might be intrinsic to the information system;
- 'White' refers to idea that it has uniform power across the frequency band for the information system. It is an analogy to the color white which has uniform emissions at all frequencies in the visible spectrum;
- 'Gaussian' because it has a normal distribution in the time domain with an average time domain value of zero;

It's a good model for satellite communication because it's free of multipath, terrain blocking, interference, ground clutter and self interference that modern radio systems encounter in terrestrial operation.

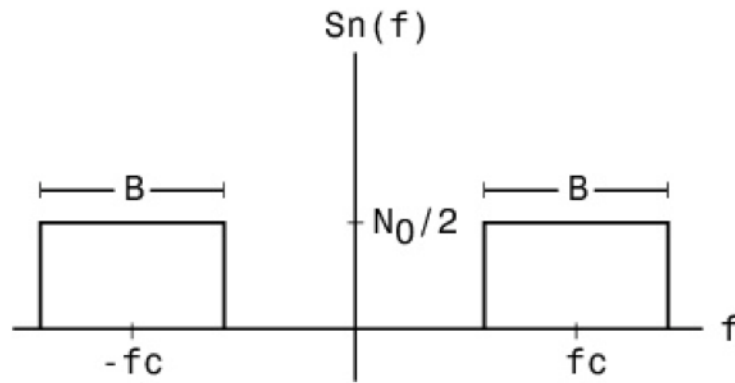


Figure 3: Real Bandpass Noise Power Spectral Density [3]

In the QPSK modulation the channel can be modelled as

$$y(t) = ax(t) + n(t), \quad (2.1)$$

where:

“y” is the received signal at the input of the QPSK receiver,

“x” is the complex modulated signal transmitted through the channel,

“a” is a channel amplitude scaling factor for the transmitted signal usually 1. And

“n” is the Additive Gaussian White Noise random variable with zero mean and variance σ^2 .

For M-PSK modulation schemes including BPSK, the symbol energy is given by:

$$E_s = R_m R_c E_b. \quad (2.2)$$

Where:

E_s = Symbol's energy per modulated bit (x), $R_m = \log_2(M)$, (for BPSK $M=2$, QPSK $M=4$, 16 QAM $M=16$ etc.,).

R_c is the code rate of the system if a coding scheme is used. In our case since no coding scheme is used $R_c = 1$, E_b is the Energy per information bit, and N_0 is the noise density, which is assumed constant for AWGN channels:

$$\frac{E_b}{N_0} = \frac{E_s}{R_m R_c N_0}. \quad (2.3)$$

σ^2 , is the noise power spectral density.

Assuming $E_s=1$ for BPSK (Symbol energy normalized to 1) $\frac{E_b}{N_0}$ can be represented as (using above equations),

$$\sigma^2 = \frac{N_0}{2}, \quad (2.4)$$

$$\frac{E_b}{N_0} = \frac{E_s}{R_m R_c N_0} = \frac{E_s}{R_m R_c 2\sigma^2} = \frac{1}{2R_m R_c \sigma^2}, \quad (2.5)$$

From the above equation the noise variance for the given E_b/N_0 can be calculated as:

$$\sigma^2 = \left(2R_m R_c \frac{E_b}{N_0}\right)^{-1}. \quad (2.6)$$

2.2 Modulation's theory

The choice of modulation technique has a direct impact on the capacity of a digital communication system. It determines the bandwidth efficiency of a single physical channel in terms of the number of bits per second per hertz (bit/s/Hz) and it is therefore important that this choice is discussed in detail.

In selecting a suitable modulation scheme for a DCM system, consideration must be given to achieving the following:

- High bandwidth efficiency;
- High power efficiency;
- Low carrier to co-channel;
- Low out-of-band radiation;
- Low sensitivity to multipath;

To optimise all these features at the same time is not possible as each has its practical limitation and also is related to the others. For example, to achieve high bandwidth efficiency one may choose to use high-level modulation. However, if this is done two consequent disadvantages are introduced. Firstly, the power efficiency of the system is reduced. Secondly, the band limited high-level modulated signal has a large envelope variation which, when the signal is passed through a power efficient nonlinear amplifier, generates large out-of-band radiation; this, in turn, introduces interference to adjacent channels. [3]

Modulation is the process of varying one or more properties of a periodic waveform, called the carrier signal (high frequency signal), with a modulating signal that typically contains information to be transmitted.

Besides, is the process of conveying a message signal, for example a digital bit

stream or an analogue audio signal, inside another signal that can be physically transmitted. Modulation of a sine waveform transforms a baseband message signal into a passband signal.

A modulator is a device that performs modulation. A demodulator (sometimes detector) is a device that performs demodulation, the inverse of modulation. A modem (from modulator–demodulator) can perform both operations.

There are two types of modulation;

2.2.1 Analogue modulation

The aim of analogue modulation is to transfer an analogue baseband (or lowpass) signal, for example an audio signal or TV signal, over an analogue bandpass channel at a different frequency, for example over a limited radio frequency band or a cable TV network channel. Common analogue modulation techniques are:

- Amplitude modulation (AM): the amplitude of the carrier signal is varied in accordance to the instantaneous amplitude of the modulating signal. Amplitude modulation of a carrier wave works by varying the strength of the transmitted signal in proportion to the information being sent;
- Frequency modulation (FM): the frequency of the carrier signal is varied in accordance to the instantaneous amplitude of the modulating signal;
- Phase modulation (PM): the phase shift of the carrier signal is varied in accordance with the instantaneous amplitude of the modulating signal. In other terms, it's and angle modulation, that alters the instantaneous phase of the carrier wave to transmit a signal; [3]

2.2.2 Digital modulation

The aim of digital modulation is to transfer a digital bit stream over an analogue bandpass channel, for example over the public switched telephone network (where a bandpass filter limits the frequency range to 300–4000 Hz), or over a limited radio frequency band. The most fundamental digital modulation techniques are based on keying:

- PSK (phase-shift keying): a finite number of phases are used. An alternative to imposing the modulation onto the carrier by varying the instantaneous frequency is to modulate the phase. This can be achieved simply by defining a relative phase shift from the carrier, usually equidistant for each required state. Therefore a two level phase modulated system, such as Binary Phase Shift Keying, has two relative phase shifts from the carrier, $+90^\circ$ or -90° . Typically this technique will lead to an improved BER performance compared to MSK. The resulting signal will, however, probably not be constant amplitude and not be very spectrally efficient due to the rapid phase discontinuities. Some additional filtering will be required to limit the spectral occupancy. Phase modulation requires coherent generation and as such if an IQ modulation technique is employed this filtering can be performed at baseband;
- FSK (frequency-shift keying): a finite number of frequencies are used as seen in

figure 4. FSK has the advantage of being very simple to generate, simple to demodulate and due to the constant amplitude can utilise a non-linear power amplifier. Significant disadvantages, however, are the poor spectral efficiency and BER performance. This precludes its use in this basic form from cellular and even cordless systems;

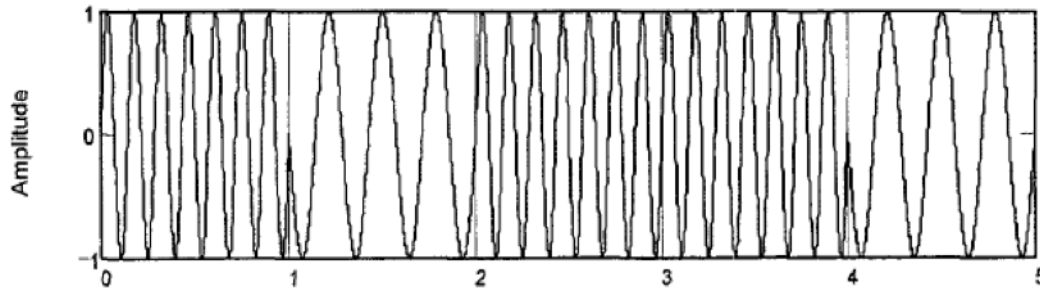


Figure 4: Binary (2 level) FSK modulation [2]

- ASK (amplitude-shift keying): a finite number of amplitudes are used;
- QAM (quadrature amplitude modulation): a finite number of at least two phases and at least two amplitudes are used;

Analogue and digital modulation facilitate frequency division multiplexing (FDM), where several low pass information signals are transferred simultaneously over the same shared physical medium, using separate passband channels (several different carrier frequencies). [3]

2.2.3 QPSK

Also known as 4-PSK or 4-QAM. For the QPSK modulation, a series of binary input message bits are generated. In QPSK, a symbol contains 2 bits. The generated binary bits are combined in terms of two bits and QPSK symbols are generated. From the constellation of QPSK modulation the symbol "00" is represented by 1, "01" by j (90 degrees phase rotation), "10" by -1 (180 degrees phase rotation) and "11" by $-j$ (270 degrees phase rotation), as shown in Figure 5.

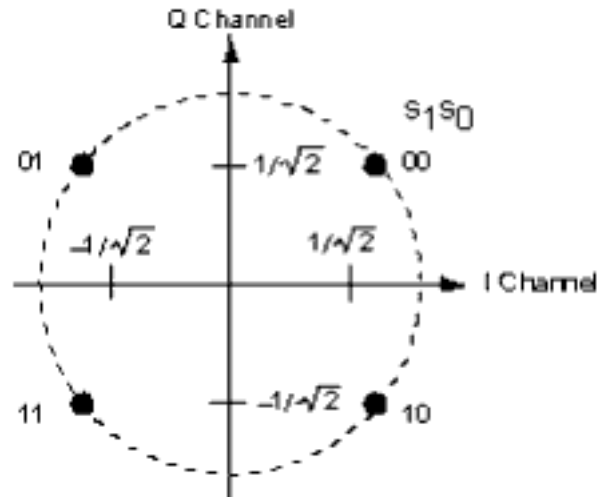


Figure 5: QPSK Constellation [24]

QPSK transmits twice the data rate in a given bandwidth compared to BPSK - at the same BER. The engineering penalty that is paid is that QPSK transmitters and receivers are more complicated than the ones for BPSK.

The implementation of QPSK is more general than that of BPSK and also indicates the implementation of higher-order PSK. Writing the symbols in the constellation diagram in terms of the sine and cosine waves used to transmit them:

$$s_n(t) = \sqrt{\frac{2E_s}{T_s}} \cos(2\pi f_c t + (2n - 1)\frac{\pi}{4}), \quad n=1,2,3,4. \quad (2.7)$$

This yields the four phases $\pi/4$, $3\pi/4$, $5\pi/4$ and $7\pi/4$ as needed.

This results in a two-dimensional signal space with unit basis functions.

$$\phi_1(t) = \sqrt{\frac{2}{T_s}} \cos(2\pi f_c t), \quad (2.8)$$

$$\phi_2(t) = \sqrt{\frac{2}{T_s}} \sin(2\pi f_c t), \quad (2.9)$$

The first basis function is used as the in-phase component of the signal and the second as the quadrature component of the signal.

Hence, the signal constellation consists of the signal-space 4 points:

$$\left(\pm \sqrt{\frac{E_s}{2}}, \pm \sqrt{\frac{E_s}{2}}\right). \quad (2.10)$$

The factors of 1/2 indicate that the total power is split equally between the two carriers.

Comparing these basis functions with that for BPSK shows clearly how QPSK can be viewed as two independent BPSK signals. Note that the signal-space points for BPSK do not need to split the symbol (bit) energy over the two carriers in the scheme shown in the BPSK constellation diagram. [2]

Although QPSK can be viewed as a quaternary modulation, it is easier to see it as two independently modulated quadrature carriers. With this interpretation, the even (or odd) bits are used to modulate the in-phase component of the carrier, while the odd (or even) bits are used to modulate the quadrature-phase component of the carrier. BPSK is used on both carriers and they can be independently demodulated.

As a result, the probability of bit-error for QPSK is the same as for BPSK:

$$P_b = Q\left(\sqrt{\frac{2E_b}{N_o}}\right). \quad (2.11)$$

However, in order to achieve the same bit-error probability as BPSK, QPSK uses twice the power (since two bits are transmitted simultaneously).

The symbol error rate is given by:

$$P_s = 2Q\left(\sqrt{\frac{E_s}{N_o}}\right) - [Q\left(\sqrt{\frac{E_s}{N_o}}\right)]^2. \quad (2.12)$$

If the signal-to-noise ratio is high (as is necessary for practical QPSK systems) the probability of symbol error may be approximated by:

$$P_s \approx 2Q\left(\sqrt{\frac{E_s}{N_o}}\right). \quad (2.13)$$

2.2.4 GMSK

Minimum shift keying (MSK) is a special case of binary continuous phase frequency shift keying (FSK) with a modulation index of 0.5 or with a frequency deviation of:

$$\Delta f = \frac{(f_2 - f_1)}{2} = \frac{1}{4T_b} \quad (2.14)$$

where f_1 and f_2 , are two discrete frequencies of the MSK signal representing logic states 1 and 0, function is easily realised.

A variant of MSK that is employed by some cellular systems (including GSM) is Gaussian Minimum Shift Keying. Again GMSK can be viewed as either frequency or phase modulation. The phase of the carrier is advanced or retarded up to 90° over the course of a bit period depending on the data pattern, although the rate of change of phase is limited with a Gaussian response. The net result of this is that depending on the Bandwidth Time product (BT), effectively the severity of the

shaping, the achieved phase change over the bit may fall short of 90° . This will obviously have an impact on the BER although the advantage of this scheme is the improved bandwidth efficiency. The extent of this shaping can clearly be seen from the 'eye' diagrams in Figure 6 below for $BT=0.3$, $BT=0.5$ and $BT=1$.

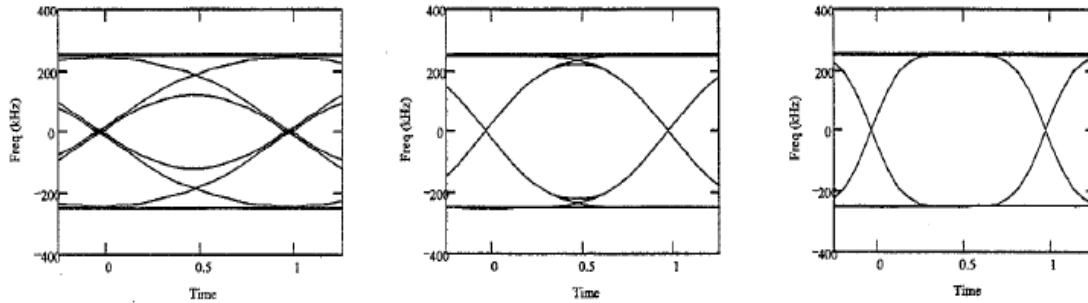


Figure 6: Eye Diagrams for GMSK with $BT=0.3$ (left), $BT=0.5$ (centre) and $BT=1$ (right).

This resultant reduction in the phase change of the carrier for the shaped symbols (ie 101 and 010) will ultimately degrade the BER performance as less phase has been accrued or retarded therefore less noise will be required to transform a zero to a one and vice versa. The principle advantages of GMSK, however, are the improved spectral efficiency and constant amplitude. The resulting signal spectrums for $BT= 0.3, 0.5, 1$ and MSK are shown below in Figure 7. [2]

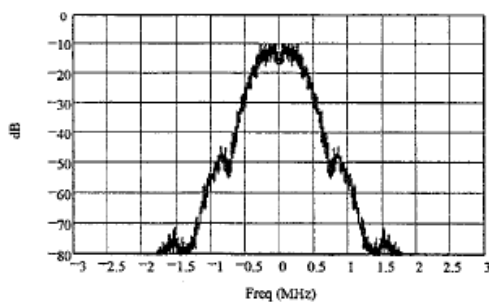


Figure 7(a): $BT=0.3$

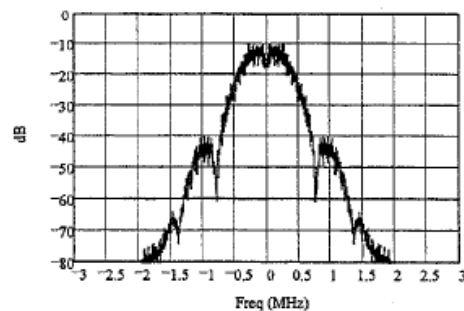


Figure 7(b): $BT=0.5$

A simple method for the modulator is to use a VCO directly with a pre-modulation Gaussian-shaped LPF as shown in Figure 8:

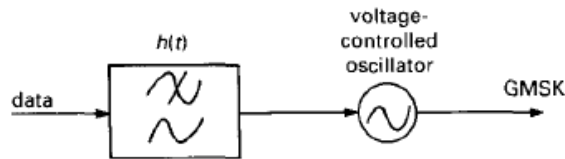


Figure 8: GMSK Modulator

The impulse response of the filter is given by:

$$h(t) = e^{-t^2/2\sigma^2T^2} / \sigma T \sqrt{2\pi}. \quad (2.15)$$

There are several advantages to the use of GMSK modulation for a radio communications system. One is obviously the improved spectral efficiency when compared to other phase shift keyed modes.

A further advantage of GMSK is that it can be amplified by a non-linear amplifier and remain undistorted. This is because there are no elements of the signal that are carried as amplitude variations. This advantage is of particular importance when using small portable transmitters, such as those required by cellular technology. Non-linear amplifiers are more efficient in terms of the DC power input from the power rails that they convert into a radio frequency signal. This means that the power consumption for a given output is much less, and this results in lower levels of battery consumption; a very important factor for cell phones. [2]

A further advantage of GMSK modulation again arises from the fact that none of the information is carried as amplitude variations. This means that is immune to amplitude variations and therefore more resilient to noise, than some other forms of modulation, because most noise is mainly amplitude based.

The Pan-European digital cellular mobile communication system (GSM) employs GMSK modulation with $BT = 0.3$ transmitting 270 kbit/s burst signal through a 200 kHz bandwidth results in a bandwidth efficiency of 1.35 bit/s/Hz for this system.

2.2.5 8PSK

8-PSK is usually the highest order PSK constellation deployed. With more than 8 phases, the error-rate becomes too high and there are better, though more complex, modulations available such as quadrature amplitude modulation (QAM). Although any number of phases may be used, the fact that the constellation must usually deal with binary data means that the number of symbols is usually a power of 2 — this allows an equal number of bits-per-symbol.

For the general M-PSK there is no simple expression for the symbol-error probability when $M > 4$. Unfortunately, it can only be obtained from:

$$P_s = 1 - \int_{-\frac{\pi}{M}}^{\frac{\pi}{M}} p_{\theta_r}(\theta_r) d\theta_r. \quad (2.16)$$

Where,

$$p_{\theta_r}(\theta_r) = \frac{1}{2\pi} e^{-2\gamma_s \sin^2 \theta_r} \int_0^\infty V e^{-\frac{(V - \sqrt{4\gamma_s \cos \theta_r})^2}{2}} dV, \quad (2.17)$$

$$V = \sqrt{r_1^2 + r_2^2}, \quad (2.18)$$

with r_1 and r_2 and Gaussian random variables. Finally, the error probability is:

$$P_s = 2Q(\sqrt{2\gamma_s \sin \frac{\pi}{M}}), \quad (2.19)$$

$$\theta_r = \tan^{-1}\left(\frac{r_2}{r_1}\right), \quad (2.20)$$

$$\gamma_s = \frac{E_s}{N_o}, \quad (2.21)$$

$$r_1 \sim N(\sqrt{E_s}, \frac{N_o}{2}), \quad (2.22)$$

$$r_2 \sim N(0, \frac{N_o}{2}), \quad (2.23)$$

The bit-error probability for M-PSK can only be determined exactly once the bit-mapping is known. However, when Gray coding is used, the most probable error from one symbol to the next produces only a single bit-error and:

$$P_b \approx \frac{1}{k} P_s. \quad (2.24)$$

(Using Gray coding allows us to approximate the Lee distance of the errors as the Hamming distance of the errors in the decoded bitstream, which is easier to implement in hardware.) [20]

2.3 Codification's theory

In communications and computer science, encoding is the process by which information from a source is converted into symbols to be communicated. Decoding is the reverse process, converting these code symbols back into information understandable by a receiver.

The Claude E. Shannon gave a formal description in 1948 to a make communication more reliable by introduced a valuable theory about the concept of information, including a good measure for the amount of information in a message. By dissecting a communication system into individual components, it is possible to improve certain aspects of the communication limitations. In particular, proper coding scheme can be utilized to improve the reliability of a communication system by reducing the error rate. In addition, suitable modulation techniques can be chosen to improve the utilization of the available bandwidth. The task of information coding theory is to detect and correct errors in the transmitted information (data) through the channel like AWGN channel. Generally, coding may be defined as source coding and channel coding. Source coding involves changing the message source to a suitable code to be transmitted through the channel. When an appropriate amount of redundancy is added to these source bits to protect them against the errors in the channel is called channel coding. The purpose of channel coding is to add controlled redundancy into the transmitted or stored information (data) to increase the reliability of transmission and lower transmission requirements. Error-correcting coding has become one essential ingredient for the latest information transmission systems. The most sophisticated codes use block code to improve the performance of data transmission.

A code is usually considered as an algorithm, which uniquely represents symbols from some source alphabet, by encoded strings, which may be in some other target alphabet. An extension of the code for representing sequences of symbols over the source alphabet is obtained by concatenating the encoded strings.

Codes are used for data compression (source coding), cryptography, error-correction (channel coding) and more recently also for network coding. In our case, we are going to apply codification for error-correction and data compression.

2.3.1 Channel coding

This enables reliable delivery of digital data over unreliable communication channels. Many communication channels are subject to channel noise, and thus errors may be introduced during transmission from the source to a receiver. Error detection techniques allow detecting such errors, while error correction enables reconstruction of the original data.

The purpose of channel coding theory is to find codes, which transmit quickly, contain many valid code words and can correct or at least detect many errors. While not mutually exclusive, performance in these areas is a trade off. So,

different codes are optimal for different applications. The needed properties of this code mainly depend on the probability of errors happening during transmission.

Deep space communications are limited by the thermal noise of the receiver which is more of a continuous nature than a burst nature. [9]

- **Linear block codes:** have the property of linearity, that is the sum of any two codewords is also a code word, and they are applied to the source bits in blocks, hence the name linear block codes. There are block codes that are not linear, but it is difficult to prove that a code is a good one without this property. They are summarized by their symbol alphabets (e.g., binary or ternary) and parameters (n, m, d_{\min}) where “n” is the length of the codeword, in symbols, “m” is the number of source symbols that will be used for encoding at once, and “ d_{\min} ” is the minimum hamming distance for the code. There are many types of linear block codes, such as cyclic codes (e.g., Hamming codes), repetition codes, parity codes, polynomial codes (e.g., BCH codes), Reed–Solomon codes, algebraic geometric codes, Reed–Muller codes and perfect codes.

Block codes rely on variable dimensions that cannot easily be visualized. The powerful (24,12) Golay code used in deep space communications uses 24 dimensions. If used as a binary code (which it usually is) the dimensions refer to the length of the codeword as defined above.

Another code property is the number of neighbours that a single codeword may have. When we increase the dimensions, the number of near neighbours increases very rapidly. The result is the number of ways for noise to make the receiver choose a neighbour (hence an error) grows as well. This is a fundamental limitation of block codes, and indeed all codes. It may be harder to cause an error to a single neighbour, but the number of neighbours can be large enough so the total error probability actually suffers.

2.3.2 Source coding

The primary task of a source codec is to represent a signal with the minimum number of (binary) symbols without exceeding an “acceptable level of distortion”, which is determined by the application.

Principle

Entropy of a source is the measure of information. Basically, source codes try to reduce the redundancy present in the source, and represent the source with fewer bits that carry more information.

Data compression that explicitly tries to minimize the average length of messages according to a particular assumed probability model is called entropy encoding.

Various techniques used by source coding schemes try to achieve the limit of Entropy of the source. $C(x) \geq H(x)$, where $H(x)$ is entropy of source (bitrate), and $C(x)$ is the bitrate after compression. In particular, no source coding scheme can be better than the entropy of the source. [9]

2.3.3 Reed-Solomon codes

Reed-Solomon error correcting codes are frequently used in coded communication systems and data storage systems, to get back data from possible errors that take place throughout transmission. Reed-Solomon codes were invented by Larry S. Reed and Gustave Solomon in 1960, who wrote "Polynomial Codes over Certain Finite Fields". Reed-Solomon codes are effective for deep fades channel and are considered as a structured sequence that is most widely used in error control codes.

The basic structure of RS code as shown in Figure 9 represented that the codeword symbols (n) is unite of two segments information symbols (k) and parity symbols ($2t$). The information symbols (k) is having message that is to be transmitted and parity symbols ($2t$) is the redundancy added to message to transmit it from source to destination without error i.e., noise.

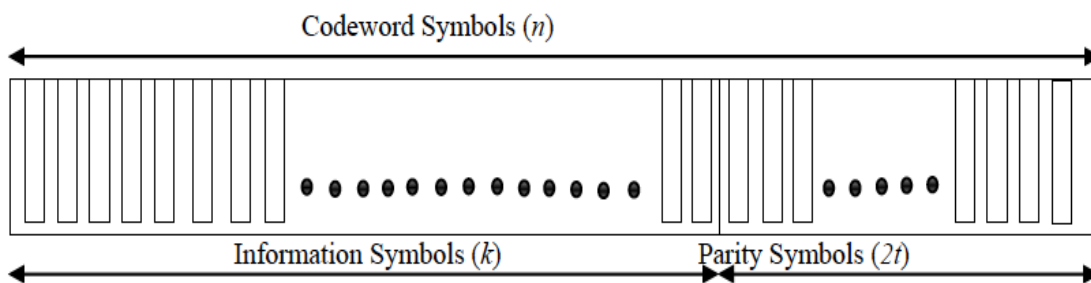


Figure 9: Structure of Reed-Solomon Code

Reed-Solomon codes are a subset of BCH codes, a linear cyclic systematic non-binary block code. Reed-Solomon codes are mainly used for burst error correction. They have very high coding rate and low complexity. At the same time, these codes are suitable for many applications including storage and transmission. RS code is a block based code and can be represented as $RS(n, k, t)$. The variable (n) is the length of the codeword symbols, (k) is the number of information symbols, (t) is the error-correction capability and each symbol contains m -bits [14]. The correlation of the symbol size (m), and the codeword symbols (n) is specified as $n = 2^m - 1$ for m -bits in one symbol, there exist $2^m - 1$ distinct symbol in one codeword, excluding the one with all zeros. The error-correction capability (t) or the maximum number of correctable random errors can be calculated by $t = (n - k)/2$. For example, the maximum number of symbol errors that RS (31, 27) decoder can correct is calculated as $(31 - 27)/2 = 2$ symbols for codeword symbols $n = 31$ and information symbols $k = 27$. The code is competent of correcting any combination of (t) or smaller number errors and can be obtained from following expressions of the error-correction capability, $t = (d_{\min} - 1)/2$.

The code minimum distance can be given by relation $d_{\min} = n - k + 1$. The code operates by oversampling a polynomial constructed from the data, thus redundant information is generated. This redundant information allows errors during transmission or storage to be corrected. The quantity and type of errors that can be corrected depends on the characteristics of the Reed-Solomon code. Codes that

realize these “optimal” error correction capabilities are called maximum distance separable (MDS) codes.

The RS (n, k, t) code parameters can be represented as follows:

Codeword symbols: $n = 2m - 1$.

Information symbols: $k = 1, 3, \dots, n - 2$.

Code minimum distance: $d_{\min} = n - k + 1$.

The error-correction capability symbols: $t = (d_{\min} - 1)/2 = (n - k)/2$.

2.3.4 Convolutional codes

The idea behind a convolutional code is to make every codeword symbol be the weighted sum of the various input message symbols. Fundamentally, convolutional codes do not offer more protection against noise than an equivalent block code. In many cases, they generally offer greater simplicity of implementation over a block code of equal power. The encoder is usually a simple circuit which has state memory and some feedback logic, normally XOR gates. The decoder can be implemented in software or firmware.

Convolutional codes are used extensively in numerous applications in order to achieve reliable data transfer, including digital video, radio, mobile communication, and satellite communication. They are used in voiceband modems (V.32, V.17, V.34) and in GSM mobile phones, as well as satellite and military communication devices.

These codes are often implemented in concatenation with a hard-decision code, particularly Reed Solomon. Prior to turbo codes, such constructions were the most efficient, coming closest to the Shannon limit. They were first introduced by Elias in 1955 as an alternative to block codes. Shortly thereafter, Wozencraft proposed sequential decoding as an efficient decoding scheme for convolutional codes, and experimental studies soon began to appear. In 1963, Massey proposed a less efficient but simpler to implement decoding method called threshold decoding. Then in 1967, proposed a maximum likelihood decoding scheme that was relatively easy to implement for codes with small memory orders.

Convolutional codes differ from block codes in that the encoder contains memory and the n encoder outputs at any time unit depend not only on the k inputs but also on m previous input blocks.

A (n, k, m) convolutional code can be implemented with a k-input, n-output linear sequential circuit with input memory m.

Typically, n and k are small integers with $k < n$, but the memory order m must be made large to achieve low error probabilities.

In the important special case when $k=1$, the information sequence is not divided into blocks and can be processed continuously.

k = number of bits shifted into the encoder at one time, the total memory in the

encoder (is sometimes called the overall constraint lengths).

n = number of encoder output bits corresponding to the k information bits.

$R_c = k/n$ = code rate.

Each encoded bit is a linear combination of the present k input bits and the previous $m \times k$ input bits. m designates the number of previous k -bit input blocks that must be memorized in the encoder. m is called the memory order of the convolutional code. To convolutionally encode data, start with k memory registers, each holding 1 input bit. Unless otherwise specified, all memory registers start with a value of 0. The encoder has n modulo-2 adders (a modulo 2 adder can be implemented with a single Boolean XOR gate, where the logic is: $0+0 = 0$, $0+1 = 1$, $1+0 = 1$, $1+1 = 0$), and n generator polynomials — one for each adder. An input bit m_1 is fed into the leftmost register. Using the generator polynomials and the existing values in the remaining registers, the encoder outputs n bits. Now bit shift all register values to the right (m_1 moves to m_0 , m_0 moves to m_{-1}) and wait for the next input bit. If there are no remaining input bits, the encoder continues output until all registers have returned to the zero state.

To decode the convolutional code, we use the Viterbi decoder. The Viterbi algorithm is a method for decoding convolutional codes. It has been counted as one of good decoding scheme up to date. This algorithm, however, is vulnerable to burst error which means a series of consecutive errors. Since most physical channels make burst errors, it can be a serious problem. This scheme, called Viterbi decoding, together with improved versions of sequential decoding, led to the application of convolutional codes to deep-space and satellite communication in early 1970s.

Noisy channels cause bit errors at receiver. Viterbi algorithm estimates actual bit sequence using trellis diagram. Commonly, its decoding algorithm is used in two different forms. This difference results from the receiving form of the bits in the receiver. Decoded information is received with hard decision or soft decision. Decoded information is explained with ± 1 on hard decision operation while soft decision decoding uses multi bit quantization. Hard decision and soft decision decoding refer to the type of quantization used on the received bits. Hard decision decoding uses 1 bit quantization on the received channel values while soft decision decoding uses multi bit quantization on the received channel values, three or four bits of precision usually. The selection of quantization levels is an important design decision because of its significant effect on the performance of the link.

There are simplifications to reduce the computational load. They rely on searching only the most likely paths. Although not optimum, they have generally been found to give good results in the lower noise environments. [17]

CHAPTER 3

3.1 Nanosatellites

As defined by Conasat (Constelação de Nanosatellites), a satellite is any object that orbits another, which is called main. Artificial satellites are spacecraft manufactured on Earth and sent on a launch vehicle. Artificial satellites can orbit around moons, comets, asteroids, planets, stars or even galaxies. After its useful life, may be orbiting satellites as space junk until reenter the Earth's atmosphere, or may be directed, through the use of thrusters, to deep space. Artificial satellites can be cataloged and grouped according to their mass, as shown below:

- Large satellites: whose weight is greater than 1000 kg;
- Average Satellites: whose weight is between 500 and 1000 kg;
- Mini Satellites, whose weight is between 100 and 500 kg;
- Micro satellites: whose weight is between 10 and 100 kg;
- Nano Satellites, whose weight is between 1 and 10 kg;
- Pico Satellites: whose weight is between 0.1 and 1 kg;
- Femto satellite: whose weight is less than 100 g.

The first model studied for this type of projects was the CubeSat, created by California Polytechnic State University and modules based on cubic edge of 10 cm, as seen in Figure 10. At baseline this pattern proved a bit critical with regard to the availability of outdoor area for placement of solar panels that generate electricity that powers the satellite subsystems, and physical space for the antennas. With the adoption of this standard with the size of 3 modules, as well as expansion of 2 more, so telescopic, besides the inclusion of 4 hinged flaps, starts to become feasible, however there is a considerable increase of the mechanical difficulties involved.

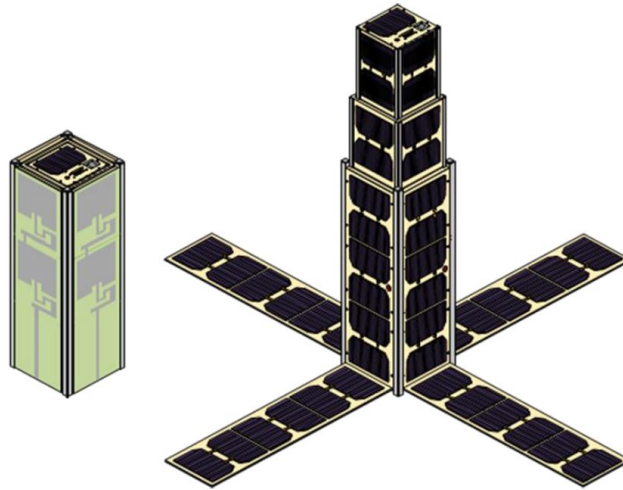


Figure 10: First Cubesat model [1]

A second alternative which appeared feasible was the standard adopted by the Space Flight Laboratory, University of Toronto, also cubic, with edges of 20 cm and maximum weight of 10 kg, as seen in Figure 11. This design allows greater latitude to circumvent the limitations in the previous model, besides presenting minor mechanical difficulties. The use of hinged flaps 4 provides enough for the antennas and solar panels additional area, thereby enabling the generation of sufficient electrical power to the expected consumption of the satellite. [14]

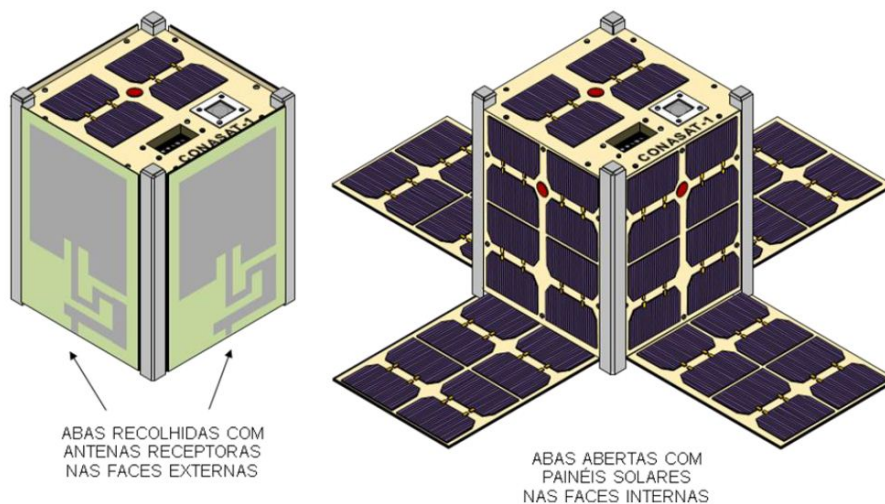


Figure 11: Second proposed Cubesat model [1]

The most recent, and which is also present in all respects viable alternative is to use the standard 3U CubeSat with a multi hinged antennas. This alternative appears to be more economical than the other, and have fewer complications constructive point of view because of the telemetry, remote control and receive

data from PCDs (micro-tape would be made alert of the electromagnetic dipole antennas while transmitting data to the receiving station would be taken in the S band frequency and in turn would use a planar antenna). The design is shown above in Figure 12.

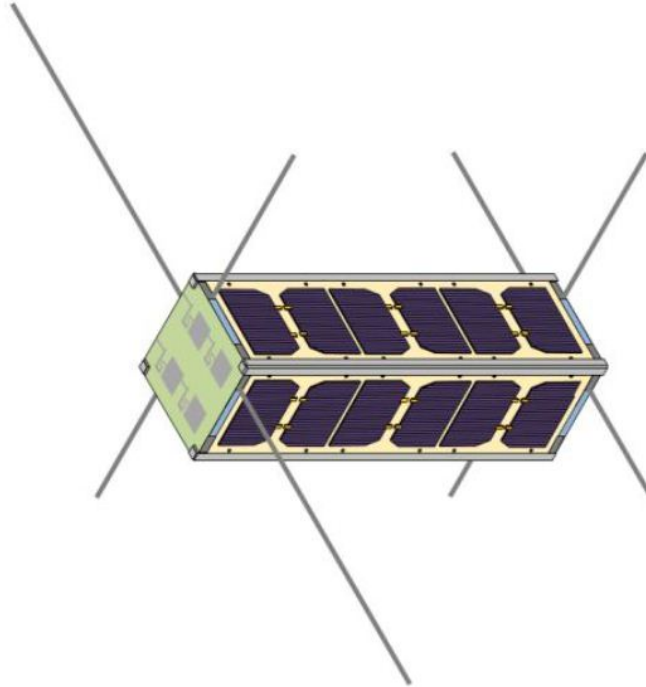


Figure 12: Actual used Cubesat model [1]

3.2 Cubesat

Started in 1999, the CubeSat Project began as a collaborative effort between Professor Jordi Puig-Suari at California Polytechnic State University and Professor Bob Twiggs at Stanford University's Space System Development Laboratory (SSDL). The purpose of the project was to provide a standard for design of picosatellites to reduce cost and development time, increase accessibility to space, and sustain frequent launches.

As mentioned above, the Cubesat specification sets strict requirements on mass and volume. These requirements are non-negotiable as they are required for the Cubesat to fit properly within, and launch correctly from inside of, the Cubesat deployer. The standard Cubesat deployer, used successfully in each Cubesat mission to date, is the Cal Poly designed Poly Picosatellite Orbital Deployer (P-POD).

The geometry of a satellite's orbit dictates a schedule of when, and for how long, the satellite is able to communicate with a fixed ground station. Cubesats are typically launched in what is called a low-earth orbit (LEO). Low earth orbits are characterized by their short range, high orbital velocity and non-geosynchronous nature.

Parameter	Value (US)	Value (metric)
Elevation	400-435 mi	650-700 km
Orbital Velocity	≈ 17,000 mi/h	≈ 27,000 km/h

Table 1: Cubesat requirements

As shown in the table 1, a Cubesat is allowed no more than 1 kg of total mass, including structure, power, electronics and payload, and no more than 100 cm² per outward face.

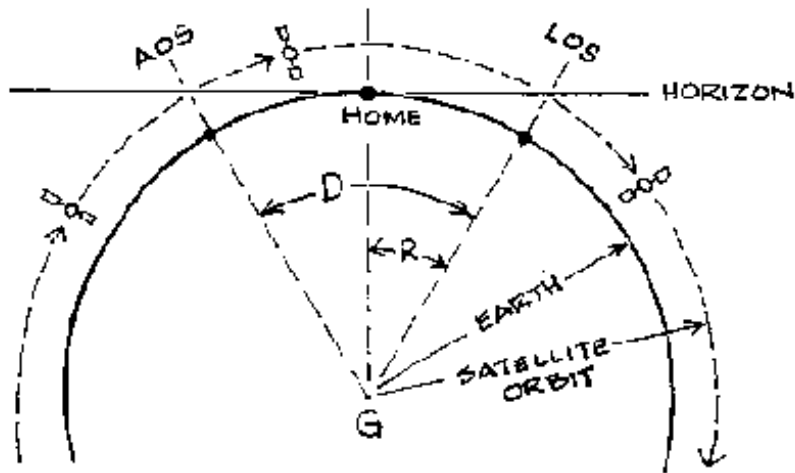


Figure 13: Communication Window in terms of AOS and LOS

The communication window for a satellite is the amount of time that a fixed ground command station can transmit to and receive signals from a satellite. The duration of this window is determined by the orbital parameters, and is defined as the length of time between AOS (acquisition of signal) and LOS (loss of signal).

3.2.1 Cubesat subsystems

The Cubesat is divided in the following subsystems that are shown in Figure 14:

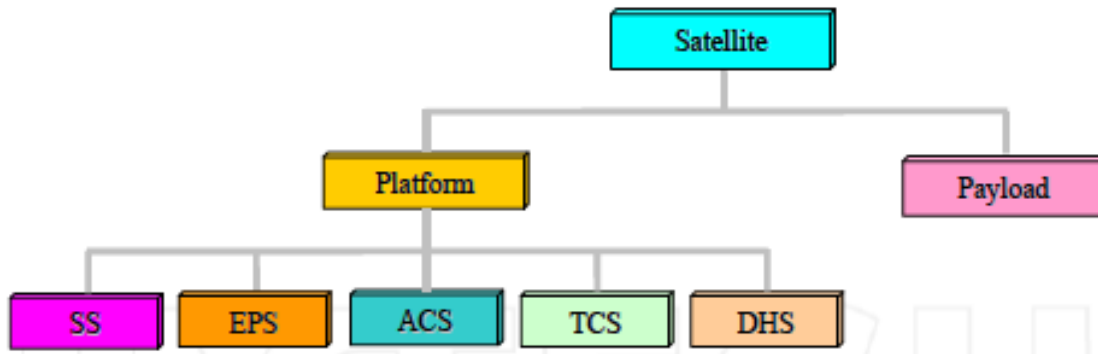


Figure 14: Satellite Cubesat subsystems

- **Altitude Control Subsystem (ACS)**

To cut down the cost of the Telecommunication CubeSat-class satellite, all the nonessential elements are suppressed. An active attitude, which consumes the energy, is avoided by using omnidirectional antenna. In the case of early launch CubeSats, the CubeSats that have adopted permanent magnets as passive attitude control, still alive and operated well. On the contrary, other Cubesats that incorporated active attitude control had many problems and was unstable. The attitude control consists of two permanent magnets placed perpendicular to Six Hysteresis rods. In fact, if one would think of the Earth as a giant bar magnet, then two parallel permanent magnets, using Neodymium Fer Bore (N35) material, aligned along an axis, would try to passively align the satellite according to the Earth's magnetic field lines. The satellite will spin around this axis and will be slowing down using six hysteresis rods (Alloy49) attached perpendicularly to this axis. The force caused by the hysteresis rods opposes the change in motion of the satellite. Also, it stabilizes the power generation and provides uniform thermal distribution to the satellite. In order to point the antenna to the earth, the antenna side of the satellite should be made as heavy as possible, acting like a gravity gradient. The antenna is mounted close to the transceiver on the center of the side opposite to the magnet side. [27]

- **Thermal Control Subsystem (TCS)**

For a small spacecraft in low Earth orbit, there are three primary sources of thermal radiation that the spacecraft will encounter, which can be seen in Figure 15.

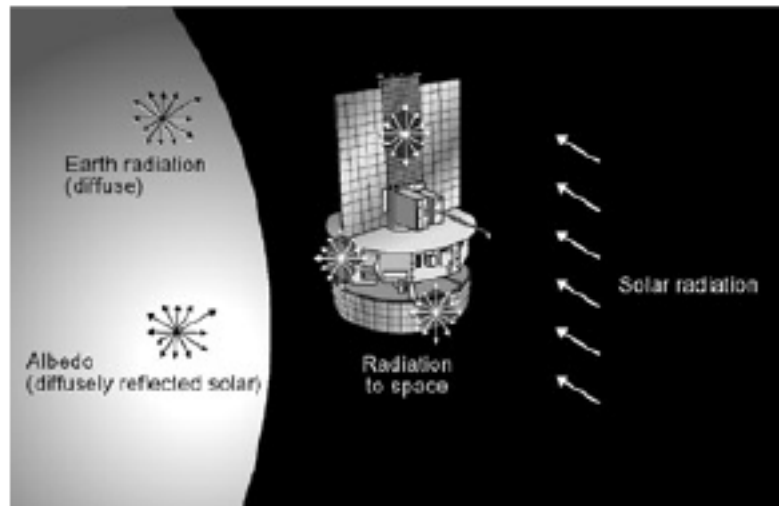


Figure 15: Space Thermal Environment

Radiation from direct sunlight, which occurs when the spacecraft is not in eclipse, is the largest factor. The fraction of sunlight that is reflected off of the earth, albedo, is also another thermal consideration for spacecraft in Earth orbit.

There is also the thermal radiation that the Earth emits at infrared wavelengths that is present regardless of eclipse.

The final environmental thermal source for the spacecraft is thermal energy emitted at infrared wavelengths from the body that the spacecraft is orbiting. For Earth, the amount of energy radiated is dependent on the region of the Earth from which sunlight is reflected, as warmer areas emit more radiation more than colder ones. [25]

- **Communication Subsystem (CS)**

The communication's subsystem's main objective is to transmit the data from onboard Cubesat to the ground station. Using a 144 Mhz uplink and a 437 MHz downlink, amateur radio bands will be used to control and receive data from the satellite.

The CubeSat communication system is composed primarily of the telemetry and command systems, which send and receive data, respectively. Analog and digital data collected by the sensors and payload of the satellite must be relayed to the ground station via the telemetry system, which is composed of a transmitter that acts much like a "modem in a computer". The microcontroller will accumulate data from the sensors and convert these inputs into a stream of 8-bit binary numbers. This numerical string is encoded into AX.25 protocol by the terminal node controller (TNC), which serves to "packetize" the information and key the transmitter. The transmitter then sends the signal to the ground station through the satellite's antenna. A radio operating in the ultrahigh frequency (UHF) band at the ground station will receive the data signal and encode the stream to a form that may be interpreted by software on a laptop.

Another vital aspect of the communication subsystem is the command/uplink portion. From the ground, moderators must be able to send commands to the system. All incoming signals from the ground station will be compared to all other inputs, and any errant signals are discarded.

The Satellite Solutions CubeSat design will implement commercially available transmitter and receiver packages that operate in UHF, and therefore, care must be taken to ensure that the correct radio-data protocol is followed for the transmission to be efficient, reliable, and robust. Also, the frequency of the signals must be transmitted within the correct FCC license regulations for the system.

Finally, for adequate communication time, the data transmission rate is desired to be at least 9,600 baud, and the amount of working amperage drawn by the communication subsystem must not exceed the available power provided by the batteries or solar cells. In the case of the communication subsystem, as shown in Figure 17, a budget of 0.75 W is needed, which represents a 33% of the total Cubesat power. [26]

- **The structural subsystem (SS)**

After placing the satellite in orbit, the satellite structure materials must protect the electronic components against the ionizing radiation. The Aluminium thickness of the satellite structure determine the life time of the satellite. Many measurements made on board various satellites allow us to know the energies of the electrons and protons trapped on various altitudes. The space agencies, like ESA (the European Space Agency), established radiation models from those measurements campaigns. From this point of view, we used ESA software called SPENVES to calculate the necessary shielding to protect the electronic components in space environment. The studies determined that the satellite will experience a total radiation dose of approximately 400 rads per month when we chose Aluminium shielding of 2 mm, taking into account the constraint of the Cubesat-class satellite Weight. The aluminium shielding of 2 mm, which will be shared between the thickness of both the satellite structure and the electronic boxes, will allow the satellite to survive nearly 13 months. [27]

- **Data handling subsystem (DHS)**

In the satellite modular architecture (Wertz & Larson, 1999), each single subsystem has a dedicated hardware and software. The Cubesat has important constraints on cost, power and mass, and especially on size. The approach that has been taken in this research consists of the integration of the maximum subsystems within the same unit taking into account that single subsystems can be setup without modifying the operation of the remaining subsystems.

As said before, the Data Handling Subsystem will integrate the Telecommunication Payload, the Telemetry/Telecommand functions as well as the active part of the thermal control subsystem. The design consists of on board computer, Sensors and Control signals, and a VHF transceiver with associated antenna.

- **Power Subsystem (PCS)**

The power system is necessary for the other CubeSat subsystems, such as the microcontroller and communication, to function. The design objectives of the power system include: providing sufficient power to the electrical subsystem, minimizing power drain from the batteries, ensuring efficient recharging of the batteries, and minimizing weight and volume. All the power divisions are shown in Figure 16.

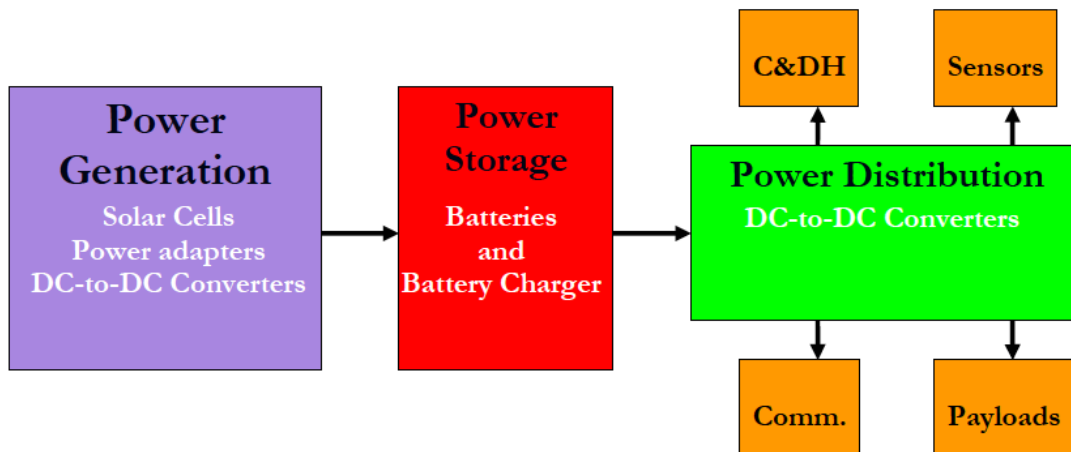


Figure 16: General Layout of the Cubesat Power Subsystem

The calculated maximum power draw on the total system is 2.25 Watts. To account for future changes and additions to other subsystems, the power was assumed to increase to 2.5 Watts. In addition, manufactures of the communication system, microcontroller, and GPS provided voltage requirements, which were 3.6 or 5 Volts. Based on the maximum power requirements from each subsystem, approximately 56%, or 1.253 Watts, of the total CubeSat power is needed for the 5 Volt subsystems and 44%, or 1 Watts, for the 3.6 Volt subsystems. Therefore, the resulting minimum currents required for the 3.6 and 5 Volt supply lines are 0.278 and 0.251 Amps. In the case of the communication subsystem, as shown in Figure 17, a budget of 0.75 W of power is needed.[4]

The chart in Figure 17 is a distribution of power based on the requirements of other subsystems, such as the CHS (C&DH), communications, sensors, and experiments.

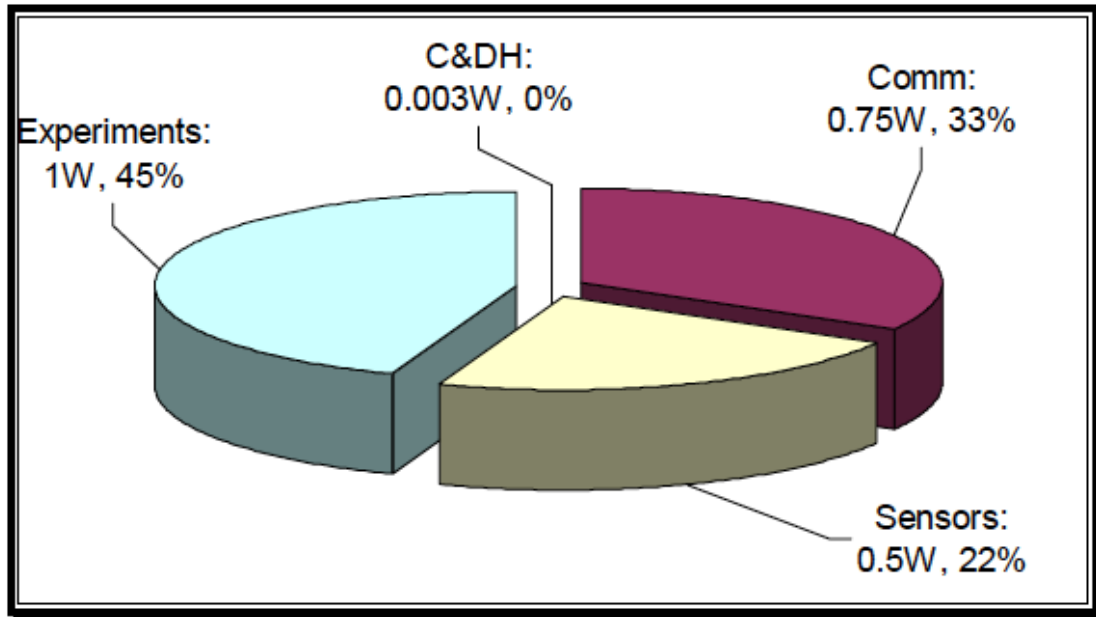


Figure 17: Power Requirement Breakdown by Subsystem

The communications window restricts telemetry and uplinking activities to many short bursts over the course of one day. Due to the short duration of availability, a high data rate is necessary.

Given the payload specification for the Cubesat, a maximum data transmission size of approximately 40 Kbytes is expected. This maximum data size, together with the limited number of passes and variable pass length, will determine a minimum baud rate required for data transmission. The possibilities are calculated below, assuming perfect transmission.

Duration	Passes	Total Time	Min Data Rate
5 min.	1	300 sec.	1.093 Kbits/sec.
5 min.	3	900 sec.	0.365 Kbits/sec.
5 min.	5	1500 sec.	0.219 Kbits/sec.
10 min.	1	600 sec.	0.547 Kbits/sec.
10 min.	3	1800 sec.	0.183 Kbits/sec.
10 min.	5	3000 sec.	0.11 Kbits/sec.

Table 2: Minimum Baud Rate Calculation [4]

In the worst case, a data rate just over 1 Kbps is necessary. Standard data transfer rates are based off of multiples of 300 bps, thus a minimum data rate of 1.2 Kbps should satisfy the conditions above requirements as long as the higher-level protocol chosen has a relatively low overhead. Higher data rates are acceptable as long as they are equally reliable.

Because of the enormous distance between the satellite and the ground command station, the probability of data packet corruption is assumed to be non-negligible. The communications protocol chosen to transmit and receive data must have provisions for providing some sort of reliability. If necessary, a simple handshaking and verification protocol may be implemented on top of an existing,

unreliable protocol.

The choice of communications subsystem electronics must be made in order to keep power consumption to an absolute minimum. Additionally, any software methods available to decrease power consumption should be exploited. Because communications is the primary consumer of power, optimizations made to decrease power consumption of this subsystem will be worth the time and effort.

The design of the power generation area includes solar cells, a power adapter, and DC-to-DC converter. The solar cells can be wired in two different configurations. In the first configuration, all the cells are wired together in series, which means that the voltage adds while the current remains constant. The second configuration has the cells wired together in parallel on each face; then, the combined cells on each face are wired in series. Note that if the output voltage from the solar cells and power adapter are within the input voltage of the battery charger, then a DC-to-DC converter may not be necessary.

The battery charger receives power and energy from the power distribution element, and outputs power to the power distribution element. Generally, the battery charger is connected directly to the battery, which in turn, is connected to the system load.

The power storage element is required to support the system load (power distribution) and recharge the batteries. The output voltage from the batteries must be matched with the input voltage required for the power distribution element. Furthermore, the batteries should support the maximum power draw. Obviously, the battery charger must be capable of charging the selected battery chemistry. In addition, the input voltage of the battery charger must be matched with output voltage from the power generation element.

These batteries must support the full functionality of the satellite, and thus power consumption must be strictly budgeted between satellite subsystems. Because communications is responsible for consuming 33% of our available power budget, every effort should be made to reduce the power consumption of this subsystem.

In order to support the load, the batteries must be able to produce the needed output energy for the period of one orbit. The output energy (to the power distribution element) is a function of power and operational percentage per orbit of each subsystem, the power distribution efficiency, and the orbital period:

$$E_{out} = \frac{T}{\eta_{pds}} \sum_{i=1}^n P_i \beta_i. \quad (3.1)$$

Where:

T is the orbital period

η_{pdc} is the efficiency of the converter in the power distribution element, P_i is the power draw from a particular subsystem and β_i is the active operational percentage per orbit for a subsystem.

The orbital period is calculated based on the altitude the CubeSat is above the Earth's surface. From Kepler's second law, the orbital period is

$$T = 2\pi \sqrt{\frac{a^3}{\mu}}, \quad (3.2)$$

where:

a is the radius from the center Earth and μ is the gravitational constant for the Earth.

The energy out of the battery depends on the capacity and voltage of the battery setup, and always needs to be greater than E_{out} .

$$E_{batt} = CV, \quad (3.3)$$

where:

C is the capacity of the battery and V is the voltage.

The number of batteries, wiring configuration, and capacity of each individual battery are adjusted to satisfy the power system design objectives while maintaining the necessary design specifications.

Furthermore, the output energy must be less than the input energy in order for the battery charger to resupply the batteries with the energy lost. In this circumstance, the energy is dependent on the orbital time in the sun and the power generated by the solar cells. [4]

CHAPTER 4

4.1 SBCD (Sistema Brasileiro de Coleta de Dados)

The applications of space technology in the solution of typical problems of a country with the geopolitical features of Brazil are the main justification for government investments in this sector. The planning of the Brazilian space activities should include the applications of space technology in the solution of problems in remote areas such as communications, environmental monitoring, surveillance Amazon, border patrol and coastal zone inventory and monitoring of natural resources, planning and supervision of land use, provision of agricultural crops, environmental data collection, the forecast weather and climate, vehicle location and development of claims and industrial processes in microgravity, in addition to defense and security the national territory. Government institutions executing activities space should work on developing systems, products, processes and methods of enabling space applications and should, where possible, pass on to private companies providing services or providing derivatives of these applications.

In order to meet the environmental diversity of the country, Brazil has designed and built two Satellites Data Collection (SCDs). Issued in 1993 (SCD-1) and 1998 (SCD-2), they allow, together with terrestrial platforms for data collection, determine the level and quality of water in rivers and reservoirs, the amount of precipitation, atmospheric pressure, the intensity of solar radiation, the air temperature and other parameters. In this system satellites act as relays messages. Thus, the communications between a platform and reception stations are established via satellites.

Nowadays the Brazilian Environmental Data Collection System is compound by the constellation satellites SCD-1, SCD-2 and CBERS-1 (Space Segment) and the various networks data collection platforms scattered throughout the national territory, by the Reception Stations in Cuiabá and Alcantara, and the Center for Mission Data Collection and Instrumentation Laboratory Meteorological (CPTEC / LIM). A more detailed information is given in the following section.

The initial network data collection platforms, the time of launch of the SCD-1, had only about 60 platforms. At the end of 2005 had already been deployed over 700 platforms, showing the growing interest user community, the operability of the system, and quality of services provided, factors that justified the investment made by the users. Consequently, increased commitment and responsibility of the INPE maintenance of the system in operating condition and performance improvement system to meet the needs of users. The SCD-2, with about eight years in operation, such as the SCD-1, also in the process of survival, with high possibility of failure severe that it will cause your loss. The physic and technical characteristics of the SCD-1 and SCD-2 satellites are shown in Table 3, and the thecnical and physic characteristics of CBERS-1 satellite are shown in Table 4. [5]

Mass	115 Kg (SCD-1) 117 Kg (SCD-2)
Dimensions	Base diameter: 100 cm Heigh: 80 cm
Stabilization by rotation	SCD-1: 120 rpm (initial) SCD-2: 34 rpm
Orbit	Circular 750 km Inclination of 25° 14 Rev/day
TT&C	Band S, ESA pattern
Nominal useful life	1 year (SCD-1) 2 years (SCD-2)
Useful charge	DCS Transponder Rx: 401,65 MHz Tx: 2,267 GHz

Table 3: SCD-1/SCD-2 technic characteristics

Stabilization	3 axes
Propulsion	16 x 1 N, 2 x 20 N
TT&C	UHF and S BAND
Useful life	2 years
Useful charge	DCS Transponder Rx: 401,635 MHz \pm 30 kHz Tx: 2267,52 MHz (S BAND), 20 dBm EIRP

Table 4: CBERS-1/CBERS-2 technic charateristics

This same concern existed regarding the CBERS-1, which was launched in October 1999 worked for about 3 years and 10 months until August 2003, when he stopped sending telemetry. Its estimated useful life (nominal) was two years. The replacement of CBERS-1 was held on 21 October 2003, with the launch CBERS-2. This new satellite presented in April 2005, a failure in a power subsystem. Since then is operating in degraded mode. Only CCD camera has been operated, the remaining Transponder Data Collection off from this date.

The environmental data collection of the platforms, are relayed by satellites and are received in Cuiabá and Alcântara stations, and afterwards they are sent to the Center Mission Data Collection (CMCD) in Cachoeira Paulista to processing, storage dissemination to users and control the satellites in orbit.



Figure 18: Constellation of Brazilian SCD satellite system [18]

The SCDs of the platforms pick up signals and relay them to a reception station and data processing located in Cuiabá (MT). From there, the data collected is sent to the city of Cachoeira Paulista (SP) and are available via the Internet, more than 80 companies and institutions of the system users. [16]

The Brazilian System of Environmental Data Collection can be arranged in following segments:

- a) Space Segment, consisting of satellites with useful data collection payload.
- b) Ground Segment Data Collection, composed by the various networks of data collection platforms, the receiving stations, the Centre Mission Data Collection (CMCD) and Instrumentation Laboratory Meteorological (LIM), the latter located in Cachoeira Paulista, Sao Paulo;
- c) Ground Segment Tracking and Control, composed by the screening and control stations of Cuiabá (MG) and Alcântara (MA), and the Center for Satellite Control (SCC) located in São José dos Campos (SP), whose main purpose is to monitor and control the satellites in orbit.

The areas that use or have used the system of data collection are listed below:

- Hydrology (ANA, Sivam);
- Weather (CPTEC INMET, meteorology state centers);
- Oceanography (drifting buoys, moored buoys), (DHN Petrobras);
- Atmospheric Chemistry;
- Quality of water (river buoys committees, municipalities, and CETESB and Management and Supervisory of water and environmental resources organs of state;
- Civil Defense (hydrologic warning systems);
- Monitoring hydroelectric level reservoirs plant (ANEEL);
- Tide Gauge Network;

- Engineering and Test (platform providers);
- Scientific research;
- Education and training;
- Environmental Monitoring (auxiliary data to determine the fire risk in the Forest Fire Detection Project);

Potential areas identified so far can be listed below:

- Monitoring of fishing boats (" Boats Monitoring System ");
- Animal Tracker (IBAMA, Research Institutes and Universities);
- Civil Defense Monitoring (slopes);
- Civil Defense (warning systems);
- Monitoring of sensitive cargo / transport;
- Environmental Monitoring (improvement of fire risk calculation with use of sensors Flammability (" fuel sensor "));

4.2 CONASAT Project

As has been said in the previous chapters, back in the 90s, the National Institute for Space Research (INPE) developed two satellites data collection (SCD-1 and SCD-2), and began operating a environmental monitoring satellite system. The development of SCDs was an important milestone for Brazilian space engineering, given that these satellites were first designed, built and operated in the country. Currently, there is a pressing need for development of new satellites, to ensure the full operation of the system Brazilian Environmental Data Collection (SBCD) , and to attend new social and economic demands, providing new services and incorporating improvements in system performance .

From this need, INPE (Instituto Nacional de Pesquisas Espaciais), in partnership with the Brazilian Space Agency (AEB), developed the CONASAT project, which is the study of a nanosatellite constellation to collect environmental data based on CubeSat standard, developed by California Polytechnic State University , in partnership with Stanford University's Space Systems Development Laboratory . The payload is set as a digital communication transponder, developed at INPE with data reception in UHF band and broadcast in S band, which enable communication between data collection platforms and receiving stations.

The model definitions and the technic Cubesat specifications for the Cubesat used in this project are explained in section 3.1 and 3.2 of this project.

CHAPTER 5

5.1 Simulation Results

In all the models, some blocks of the transmitter, channel, and receiver are set repeatedly.

5.1.1 Transmitter

- **Random integer Generator:** Generate random uniformly distributed integers in the range $[0, M-1]$, where M is the M-ary number.
- **QPSK/GMSK/ 8-PSK Modulator Baseband:** Modulates the input signal using the quaternary phase shift keying method
- **Raised Cosine Transmit Filter:** Upsample and filter the input signal using a normal or square root raised cosine FIR filter.
- **Oscillator:** It's defined by a sinus and cosinus wave.

5.1.2 Channel

- **AWGN Channel:** Add white Gaussian noise to the input signal. The input signal can be real or complex. This block supports multichannel processing. When using either of the variance modes with complex inputs, the variance values are equally divided among the real and imaginary components of the input signal.

5.1.3 Receiver

- **Raised Cosine Receive Filter:** Filter the input, and, if selected, downsample, using a normal or square root raised cosine FIR filter;
- **QPSK/GMSK/8-PSK Demodulator Baseband:** Demodulate the input signal using the quaternary phase shift keying method;
- **Error Rate Calculation:** Compute the error rate of the received data by comparing it to a delayed version of the transmitted data. The block output is a three-element vector consisting of the error rate, followed by the number of errors detected and the total number of symbols compared. This vector can be sent to either the workspace or an output port. The delays are specified in number of samples, regardless of whether the input is a scalar or a vector. The inputs to the 'Tx' and 'Rx' ports must be scalars or column vectors. The 'Stop simulation' option stops the simulation upon detecting a target number of errors or a maximum number of symbols, whichever comes first;

5.1.4 QPSK Model

In this case, the Random Integer Generator is set to $M=4$, in order to create a signal 4-PSK (QPSK). The sample time is set to $1e^{-7}$. At this point we have a low-pass signal of 4 bits, as shown in Figure 22(a). The Square Root block filters and upsamples the signal. The upsampling rate is set to $N=28$, which will change the sample time in the next steps to $1e^{-7}/28=3.5714e^{-09}$. The oscillator transforms the signal into a pass-band signal, with the centre in 70 MHz, as shown in Figure 23 (spectrum analyzer). All this blocks are shown in Figure 19. The input signal power of the AWGN Channel block is set to the same value, calculated with the variance just before the block. As shown in the Figure 20, in this case is set to 0.01785, which fits the 0.75 W theoretically needed in the Cubesat's communication system. After the channel, the oscillator transforms the signal again into a low-pass signal, the Raised Cosine Receive Filter filters and downsamples the signal, forcing again the sample rate to be $1e^{-7}$. As it's clear in the Figure 22(b), the signal after the demodulator matches perfectly with the expected result, it just have a irrelevant distortion, which is the difference between Figure 22 (a) and Figure 22(b). The receiver blocks are shown in Figure 21. After the demodulator, we use the scope to calculate the delay in the received signal, in order to compare the exact sample of the received signal with its original sent sample. In the QPSK the sample delay was just 9 samples. The signal to workspace block allows us to send the data to the workspace. This let the program Bertool from Matlab import the BER results from the model and build a graphic like the one shown in Figure 24.

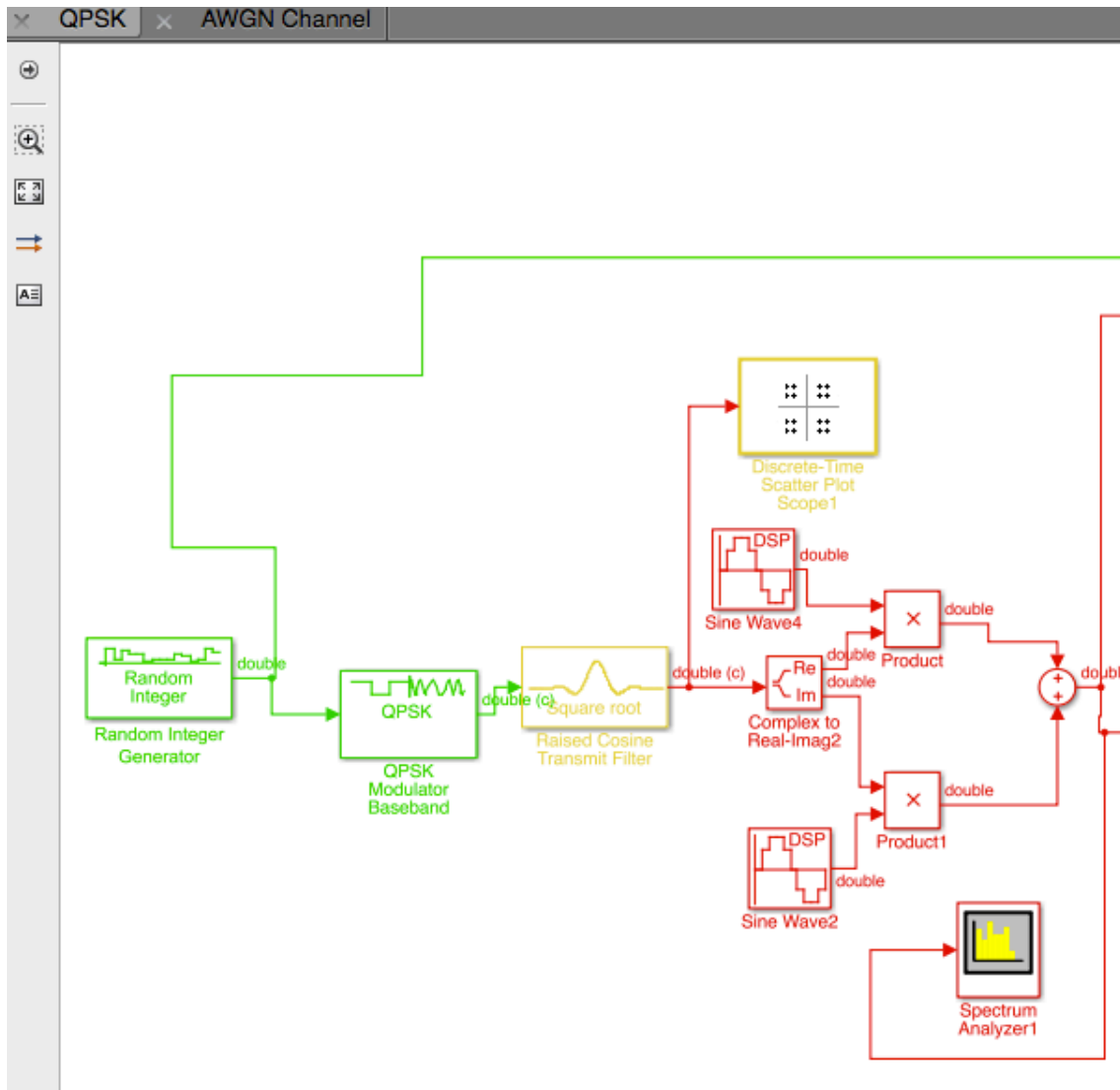


Figura 19: QPSK Simulation Model (Transmitter)

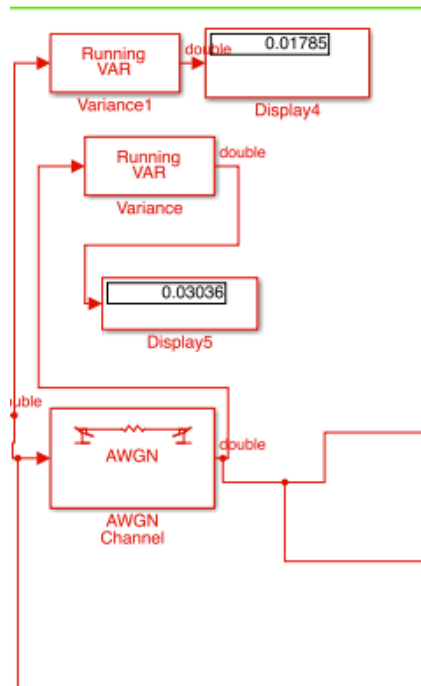


Figura 20: QPSK Simulation Model (AWGN channel)

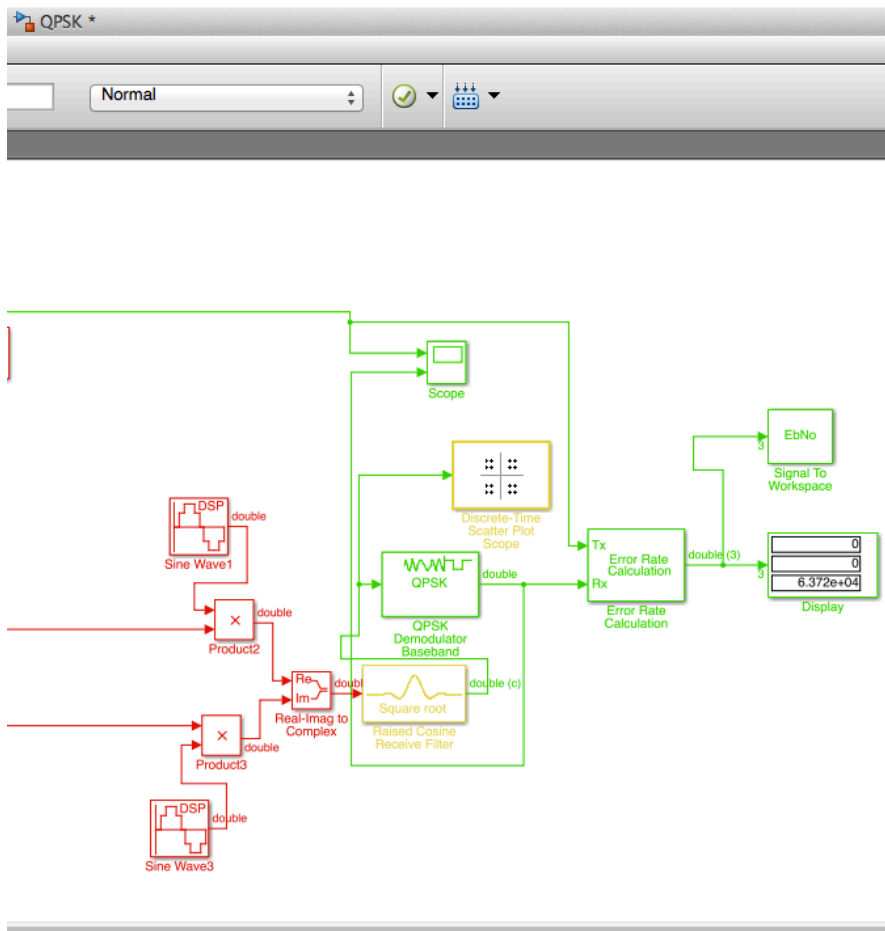


Figura 21: QPSK Simulation Model (Receiver)

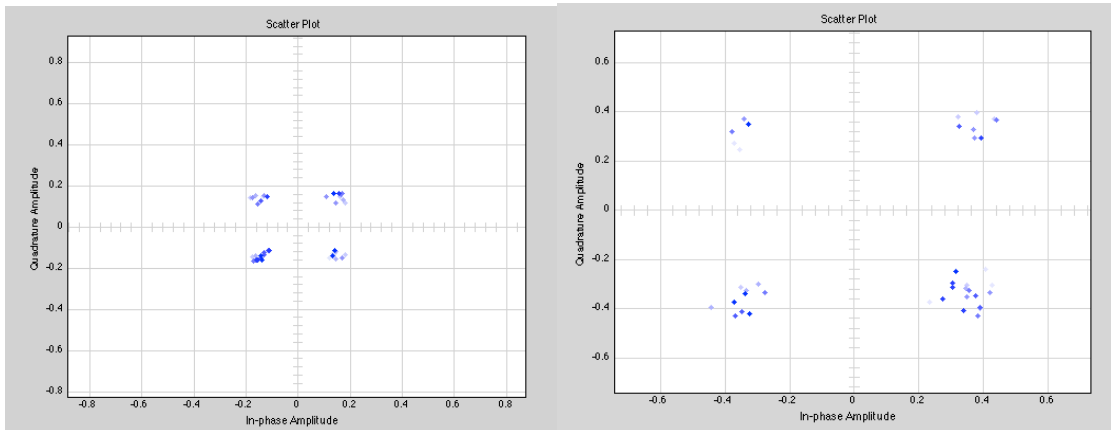


Figure 22(a): signal constellation after Raised Cosine Transmit Filter

Figure 22(b): signal constellation after Raised Cosine Receive Filter

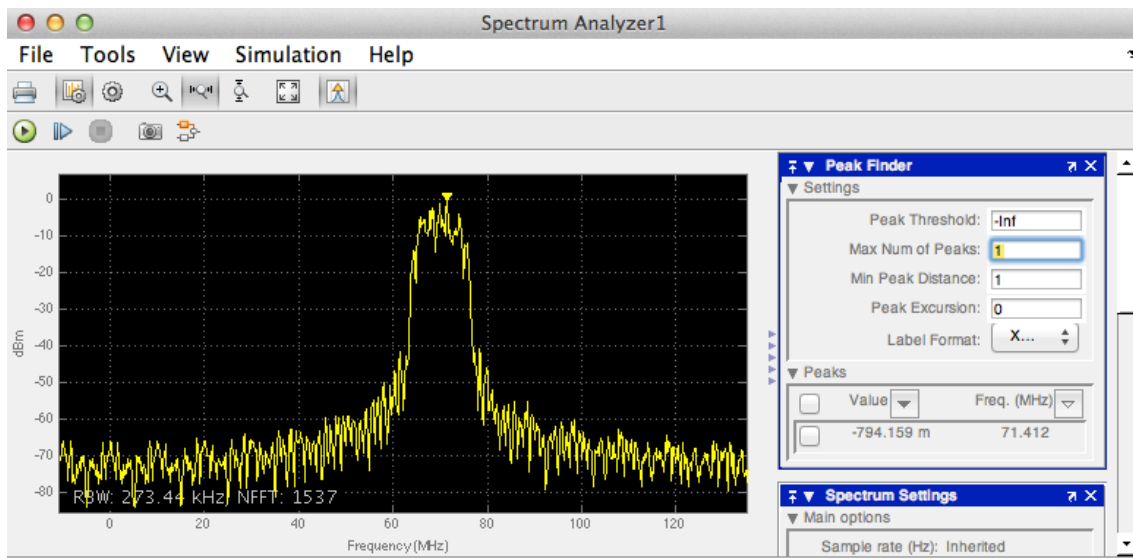


Figure 23: Spectrum Analyzer Results

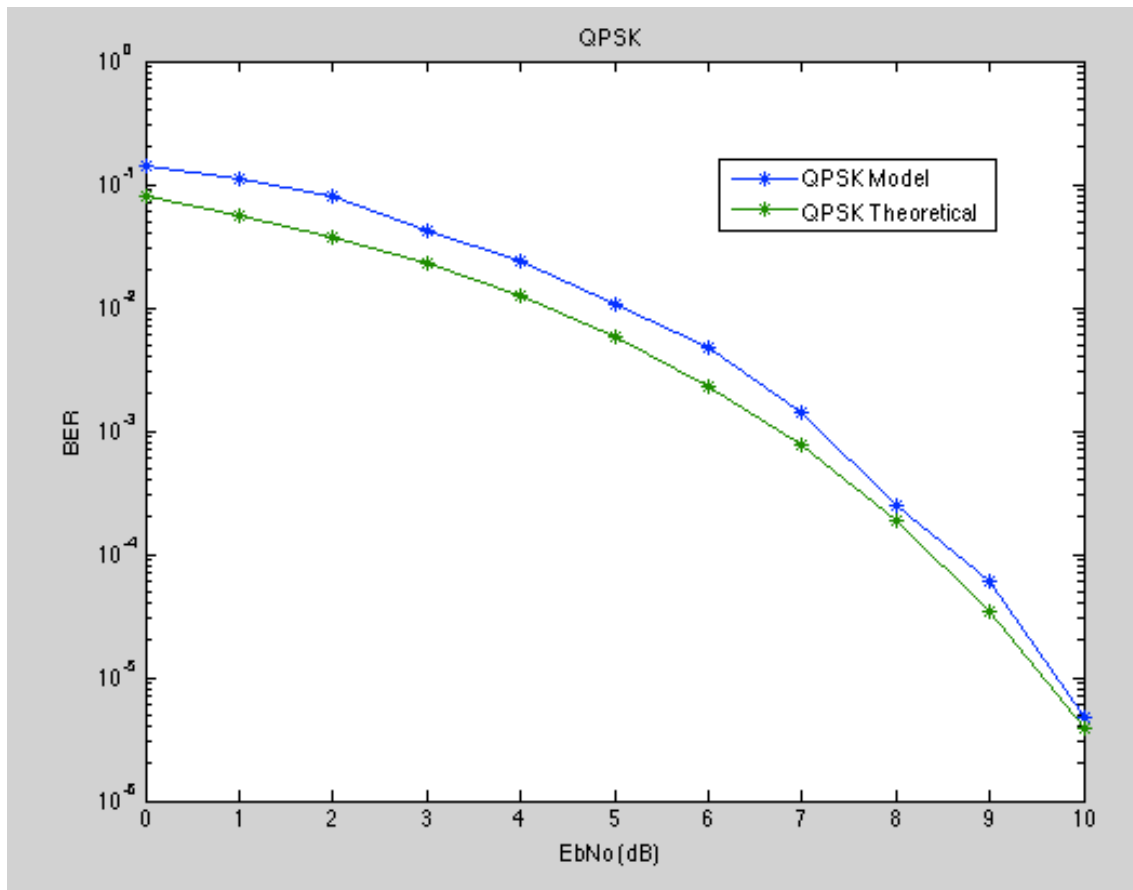


Figure 24: BER comparative between QPSK theoretic and the model

In the Figure 24 of the BER comparative, is shown that the model results are very close to the theoretical ones. The simulated model stands just 0.5 dB above the theoretical values, which is very good result.

5.1.5 8PSK Model

In this case, the Random Integer Generator is set to $M=8$, in order to create a signal 8-PSK. The sample time initially is set to $1e-7$. At this point we have a low-pass signal of 8 bits, as shown in Figure 26(a). The Square Root block filters and upsamples the signal. The upsampling rate is set to $N=28$, which will change the sample time in the next steps to $1e-7/28= 3.5714e-09$. The oscillator transforms the signal into a pass-band signal, with the centre in 70 MHz, as shown in Figure 25 (spectrum analyzer). The input signal power of the AWGN Channel block is set to the same value, calculated with the variance just before the block. As shown in the figure, in this case is set to 0,01783, which fits the 0.75 W theoretically needed in the Cubesat's communication system. After the channel, the oscillator transforms the signal again into a low-pass signal, the Raised Cosine Receive Filter filters and downsamples the signal, forcing again the sample rate to be $1e-7$. As it's clear in

the Figure 26(b), the signal after the demodulator matches with the expected result, with a minimum addition of distortion. After the demodulator, the scope allows to calculate the delay in the received signal, in order to compare the exact sample of the received signal with its original sent sample. In the 8PSK the sample delay was just 9 samples. The signal to workspace block allows us to send the data to the workspace. This let the program Bertool, import the BER results and build a graphic like the one shown in Figure 30.

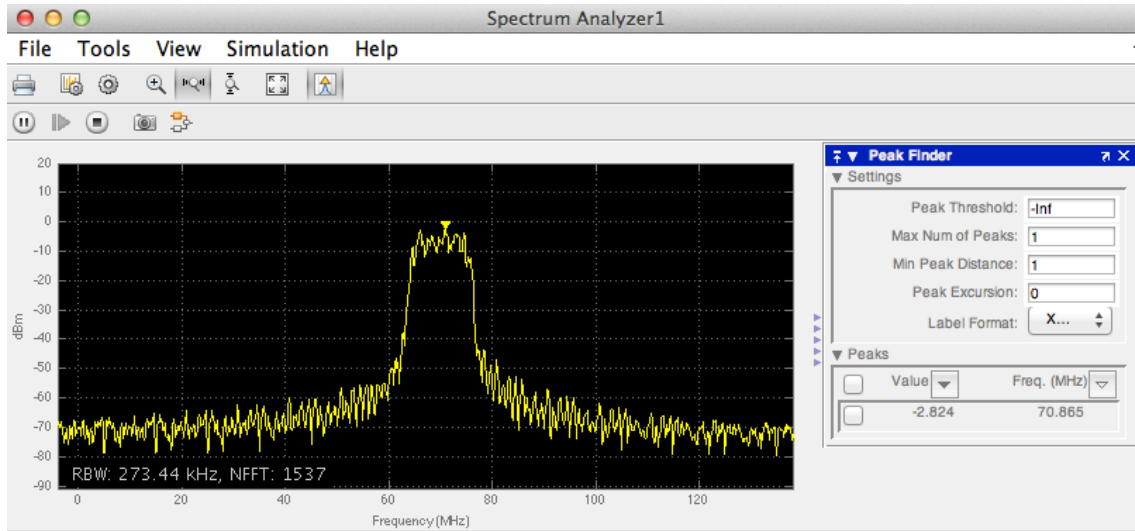


Figure 25: Spectrum Analyzer Results

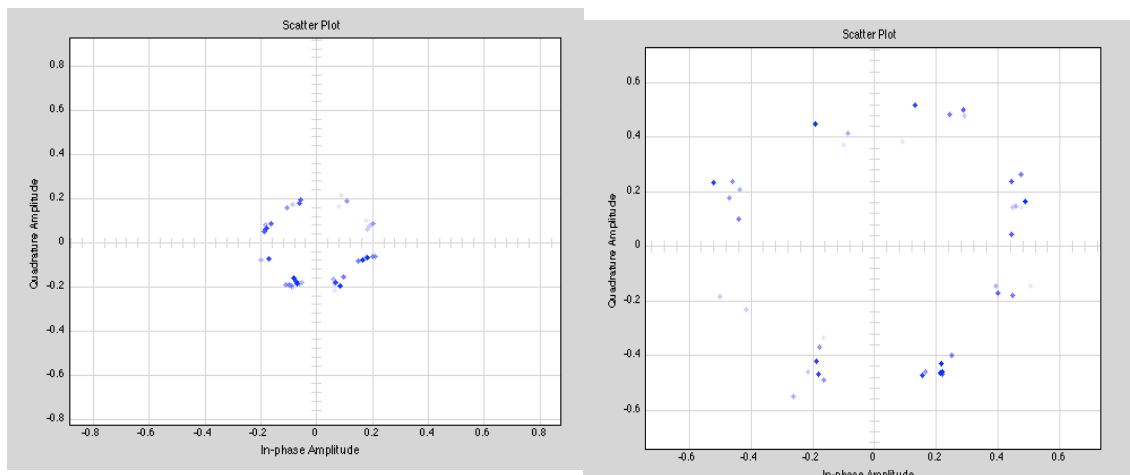


Figure 26(a): signal constellation after Raised Cosine Transmit Filter

Figure 26(b): signal constellation after Raised Cosine Receive Filter

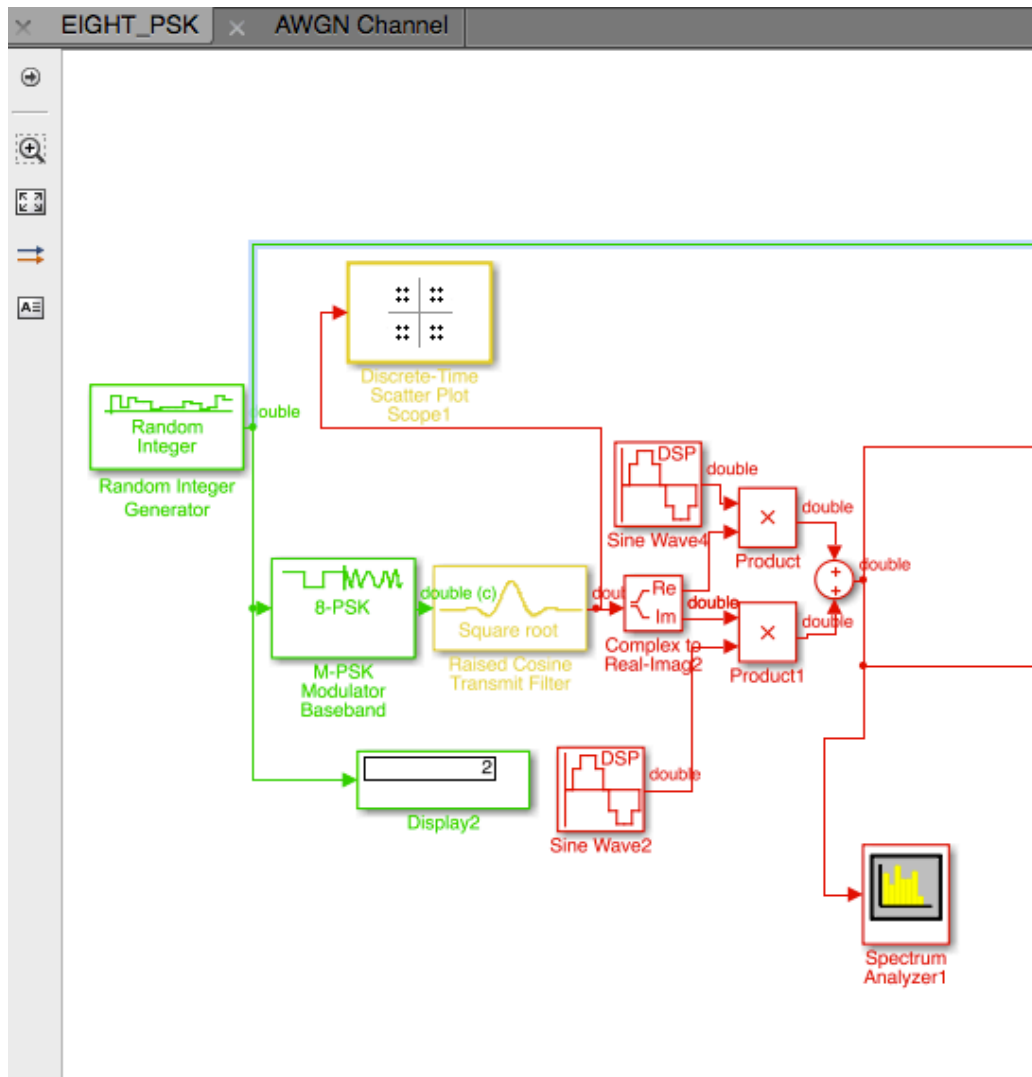


Figure 27: 8-PSK Simulation Model (Transmitter)

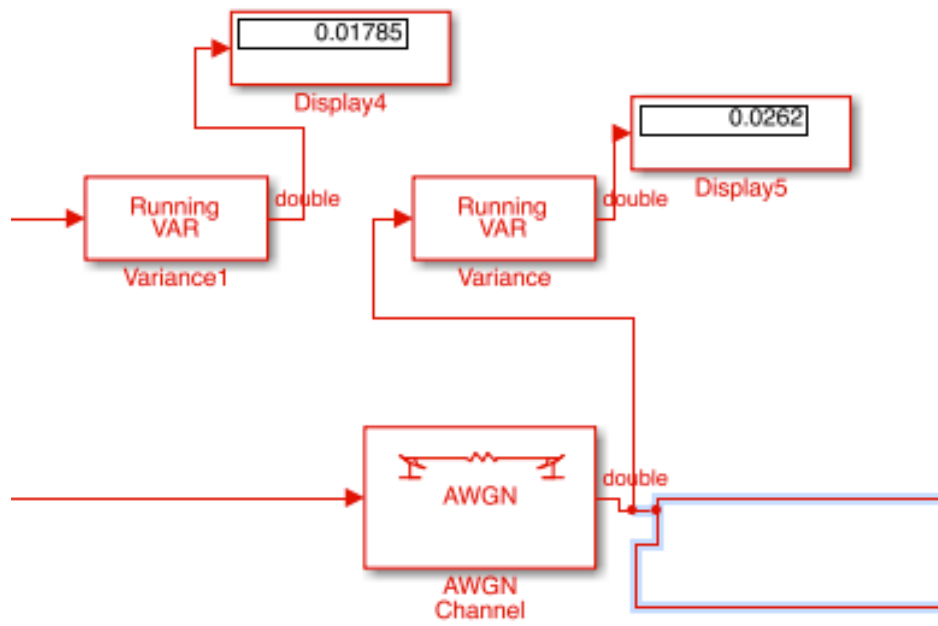


Figura 28: 8PSK Simulation Model (AWGN Channel)

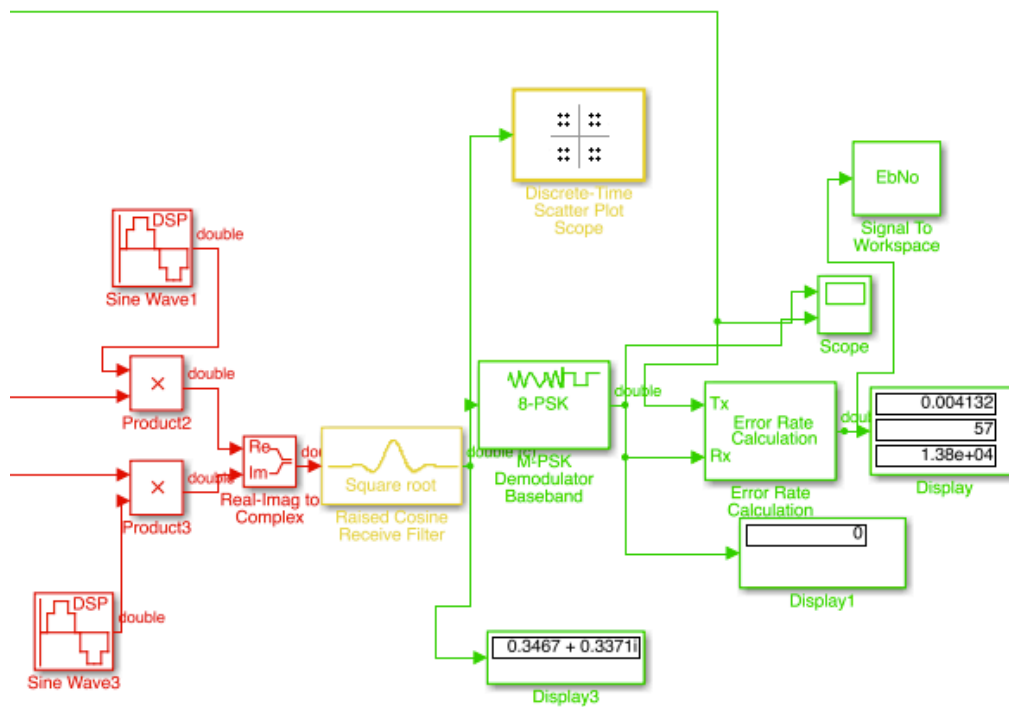


Figura 29: 8PSK Simulation Model (Receiver)

In the Figure 30 of the BER comparative, is shown that the model results are very close to the theoretical ones. The simulated model stands just 1 dB above the theoretical values, which is an acceptable result.

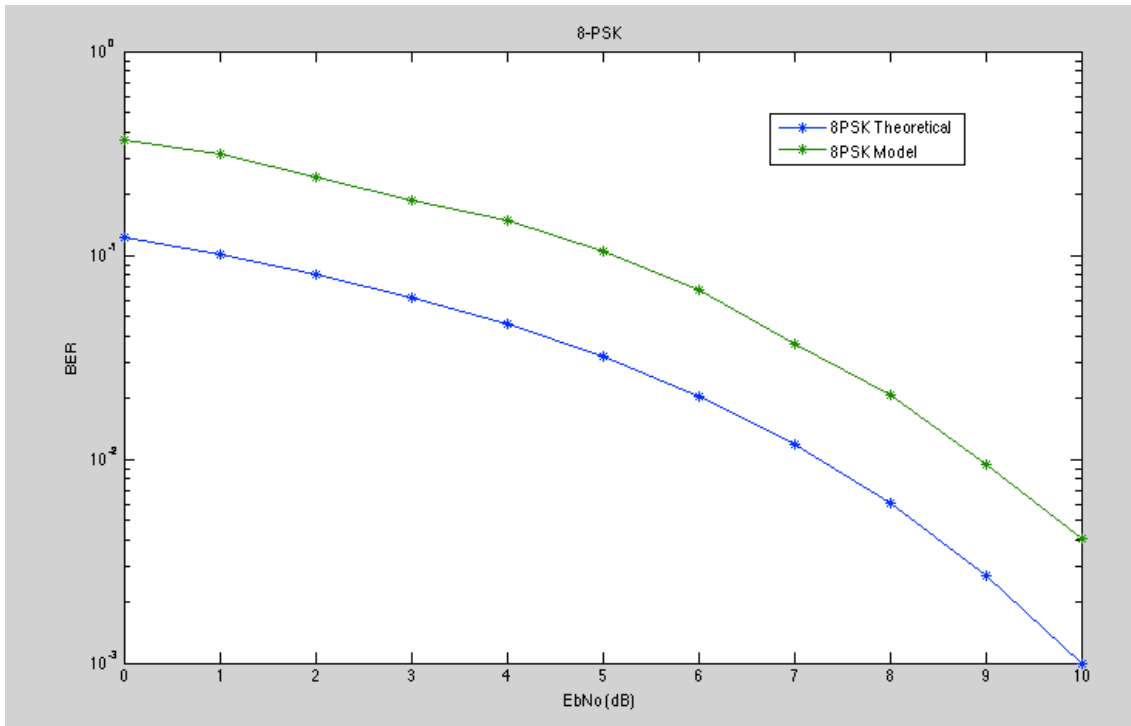


Figure 30: 8-PSK Ber comparative

5.1.5 GMSK Model

In this case, the Random Integer Generator is set to $M=8$, in order to create a signal 8-PSK. The sample time initially is set to $1e^{-7}$. The Square Root block filters and upsamples the signal. The upsampling rate is set to $N=28$, which will change the sample time in the next steps to $1e^{-7}/28 = 3.5714e^{-09}$. The oscillator transforms the signal into a pass-band signal, with the centre in 70 MHz, as shown in Figure 31 (spectrum analyzer). The input signal power of the AWGN Channel block is set to the same value, calculated with the variance just before the block. As shown in the figure, in this case is set to 0.5001, which is nearer than the QPSK and 8-PSK models, to the 0.75 W value theoretically needed in the Cubesat's communication system. However, it's still under the maximum limit, so it's a good result. After the channel, the oscillator transforms the signal again into a low-pass signal, the Raised Cosine Receive Filter filters and downsamples the signal, forcing again the sample rate to be $1e^{-7}$. After the demodulator, the scope allows to calculate the delay in the received signal, in order to compare the exact sample of the received signal with its original sent sample. In the GMSK the sample delay is 17 samples. It's almost twice the delay of the QPSK and 8 PSK models. The signal to workspace block allows us to send the data to the workspace. This block allows the program Bertool from Matlab, import the BER results and build a graphic like the one shown in Figure 35.

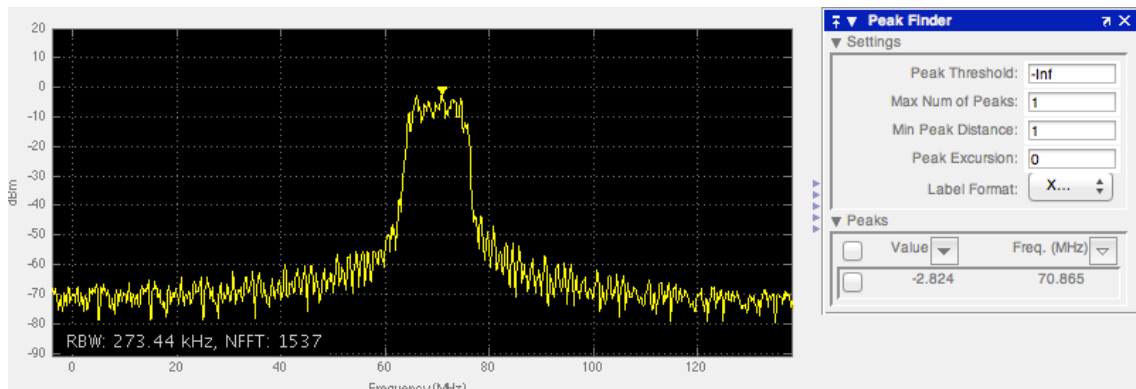


Figure 31: Spectrum Analyzer results

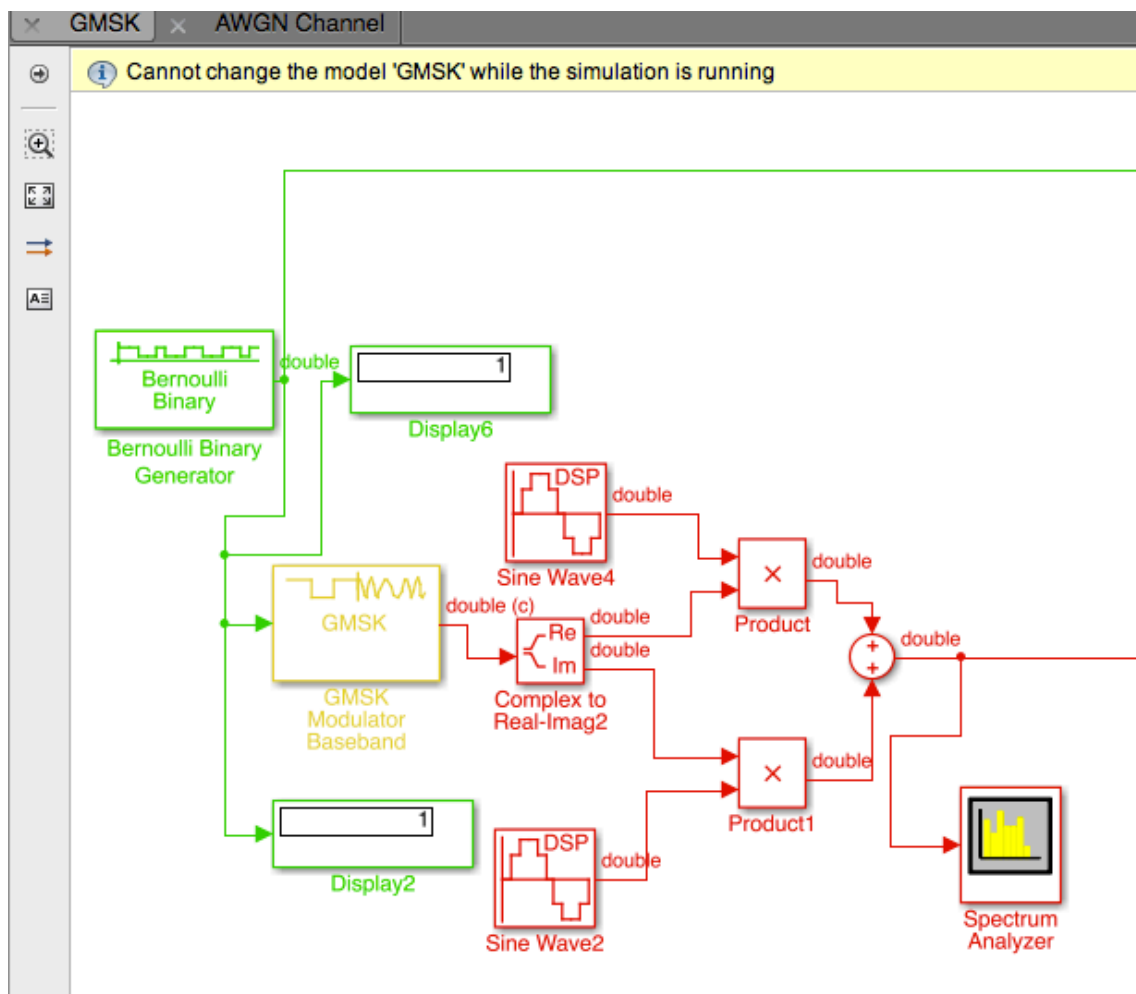


Figure 32: GMSK Simulation Model (Transmitter)

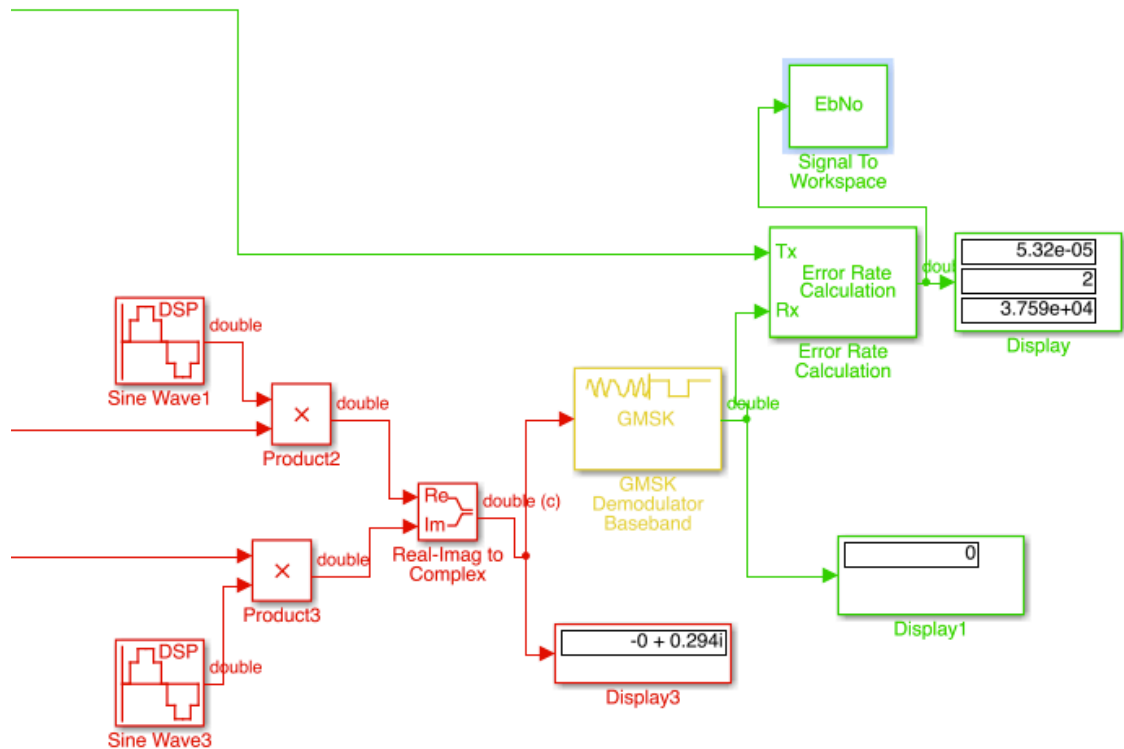


Figure 34: GMSK Simulation Model (Receiver)

In the Figure 35 of the BER comparative, is shown that the model results are very close to the theoretical ones, almost the same values. The simulated model stands just 0.1 dB above the theoretical values, which is a optimum result.

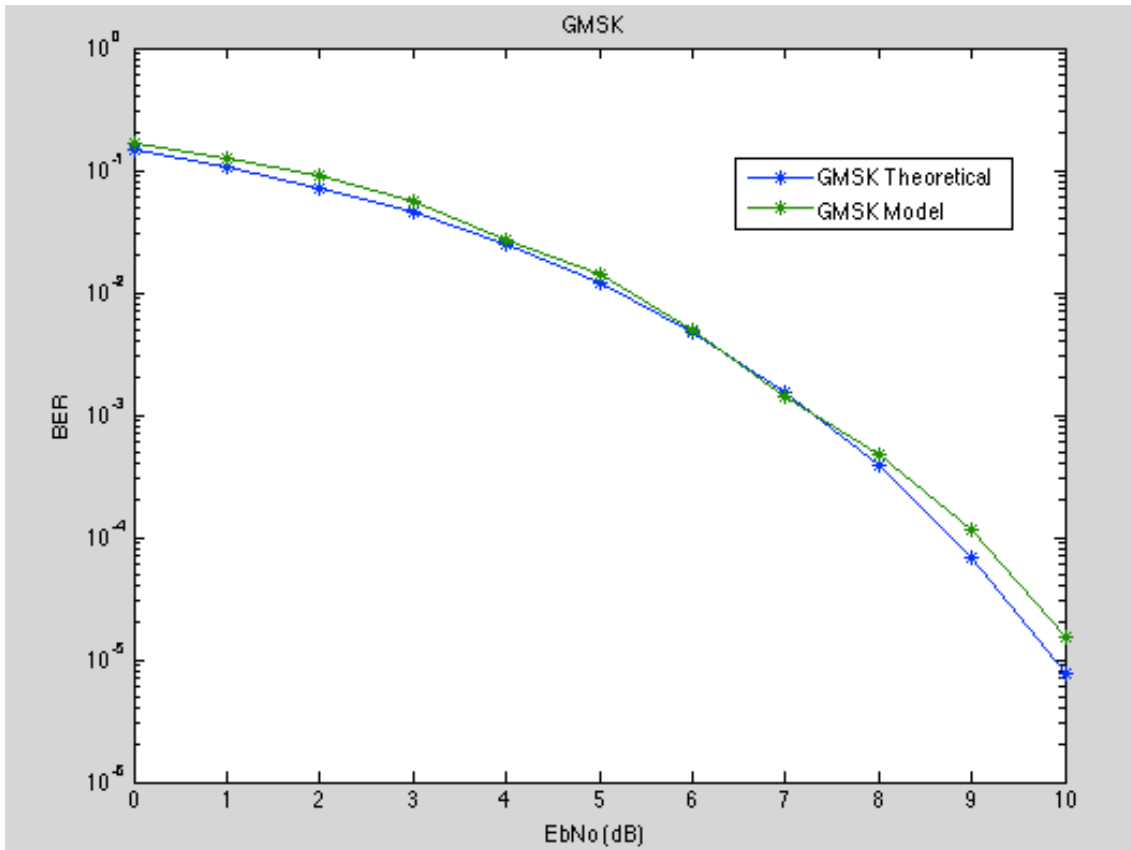


Figure 35: GMSK BER comparative

5.1.6 QPSK with convolutional encoding

For the QPSK with convolutional encoding, the model starts the same way the model without coding does. The Random Integer Generator is configured to produce an $M=4$ signal. The sample time initially is set to $1e^{-7}$. The first change from the previous models is that we use a Integer to Bit converter, because the convolutional encoder needs the signal at the input to be binary.

Due to the QPSK signal we are working with, we have a 2 bit per integer signal. The next block is the convolutional Encoder, which convolutionally encodes binary data.

We use a Convolutional (7,133,171) code.

At this point we have a low-pass signal of 4 bits. From here, the model follows the same steps as the previous models. The Square Root block filters and upsamples the signal. The upsampling rate is set to $N=28$, which will change the sample time in the next steps to $1e^{-7}/28 = 3.5714e^{-09}$. The oscillator transforms the signal into a pass-band signal, with the centre in 70 MHz, as shown in Figure 35 (spectrum analyzer). The input signal power of the AWGN Channel block is set to the same value, calculated with the variance just before the block. As shown in the Figure 36,

in this case it is set to 0.01751, which is far lower than the 0.75 W value theoretically needed in the Cubesat's communication system. After the channel, the oscillator transforms the signal again into a low-pass signal, the Raised Cosine Receive Filter filters and downsamples the signal, forcing again the sample rate to be $1e^{-7}$. After the QPSK demodulator, we have an integer to bit converter, because the Viterbi decoder demands a binary input. After that comes the Viterbi decoder. The reasons to use this decoder are well explained in the Chapter 2 (2.3.4) of this text. In this model QPSK with convolutional codification the sample delay just before the Error Rate Calculation Block is 26 samples. Almost twice the delay of the GMSK, and three times the delay of QPSK and 8 PSK models.

The signal to workspace block allows us to send the data to the workspace. This let the program Bertool, import the BER results and build a graphic like the one shown in Figure 40.

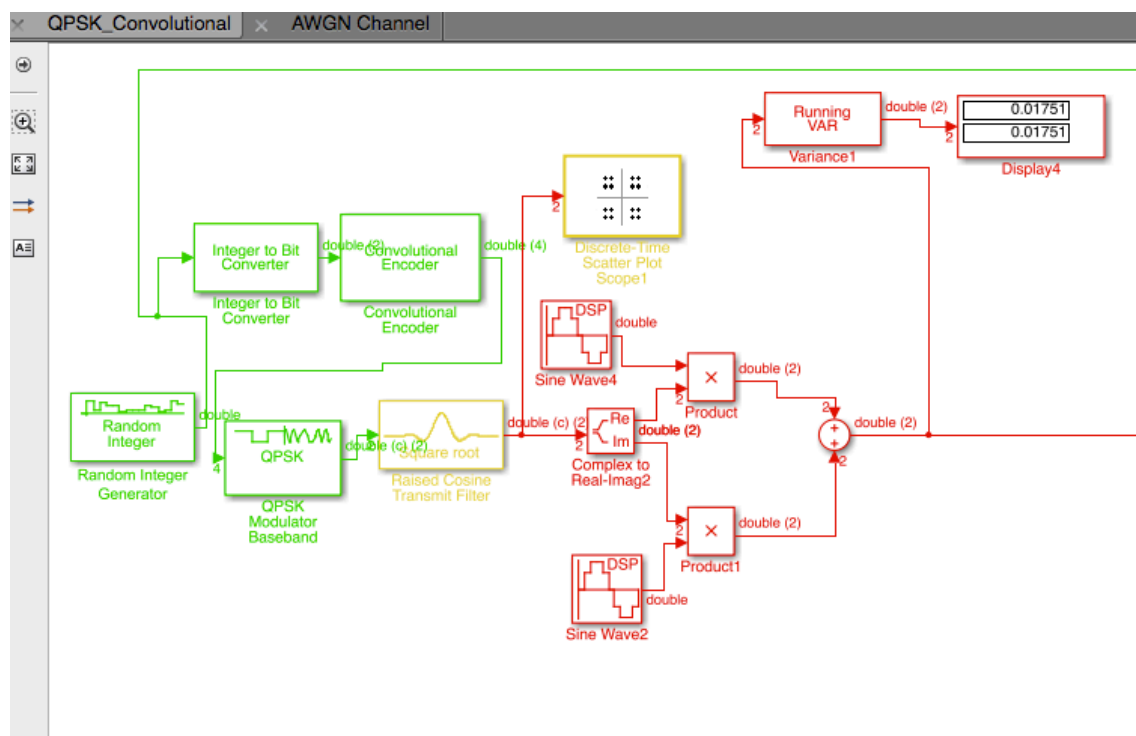


Figure 36: QPSK with convolutional encoding Simulation Model (Transmitter)

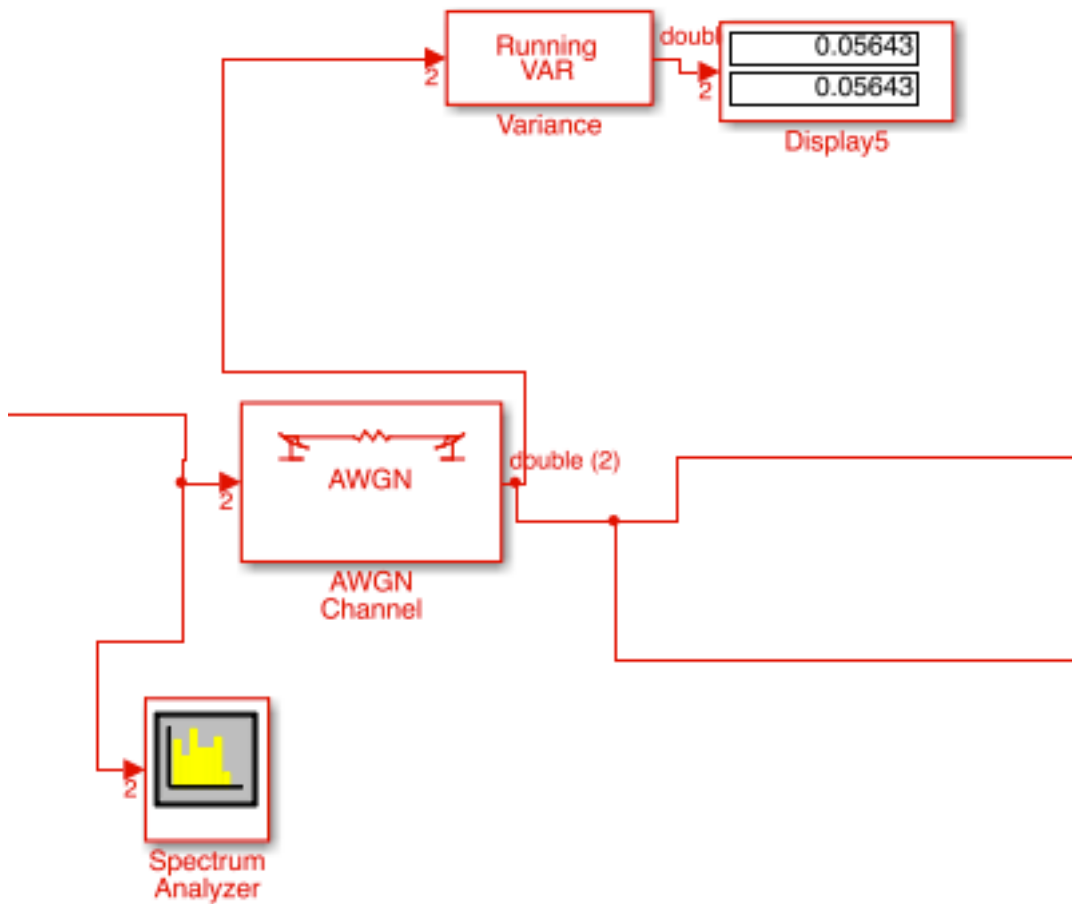


Figure 37: QPSK with convolutional encoding Simulation Model (Transmitter)

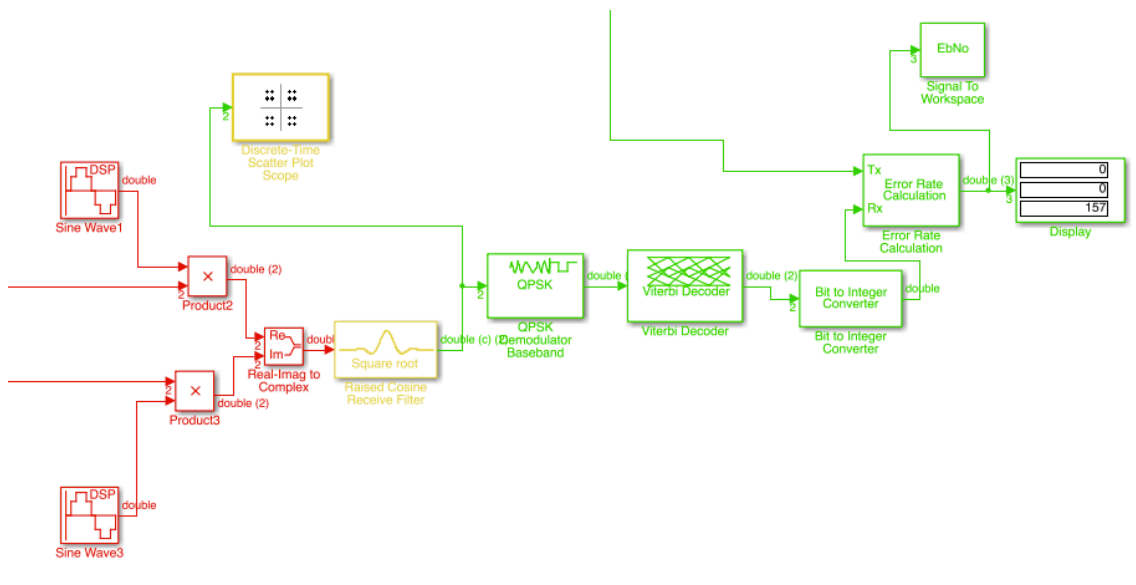


Figure 38: QPSK with convolutional encoding Simulation Model (Receiver)

As shown in Figure 39 the signal is composed by the peak, centred in 70 MHz. It's not shown in the figure but it has its image in the -70 MHz. It shows that the signal that is going through the channel is the right one. A Gaussian signal centered in 70 MHz and with no aliasing or interference.

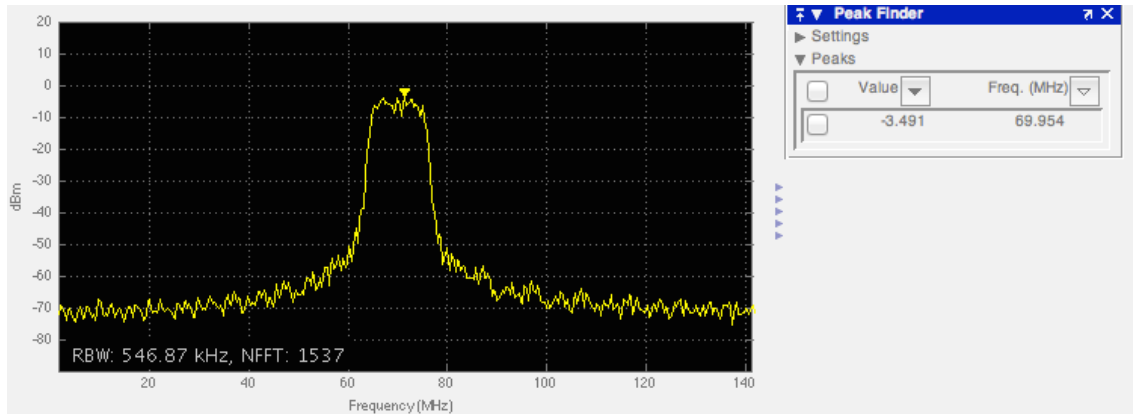


Figure 39: QPSK with convolutional encoding spectrum before AWGN channel

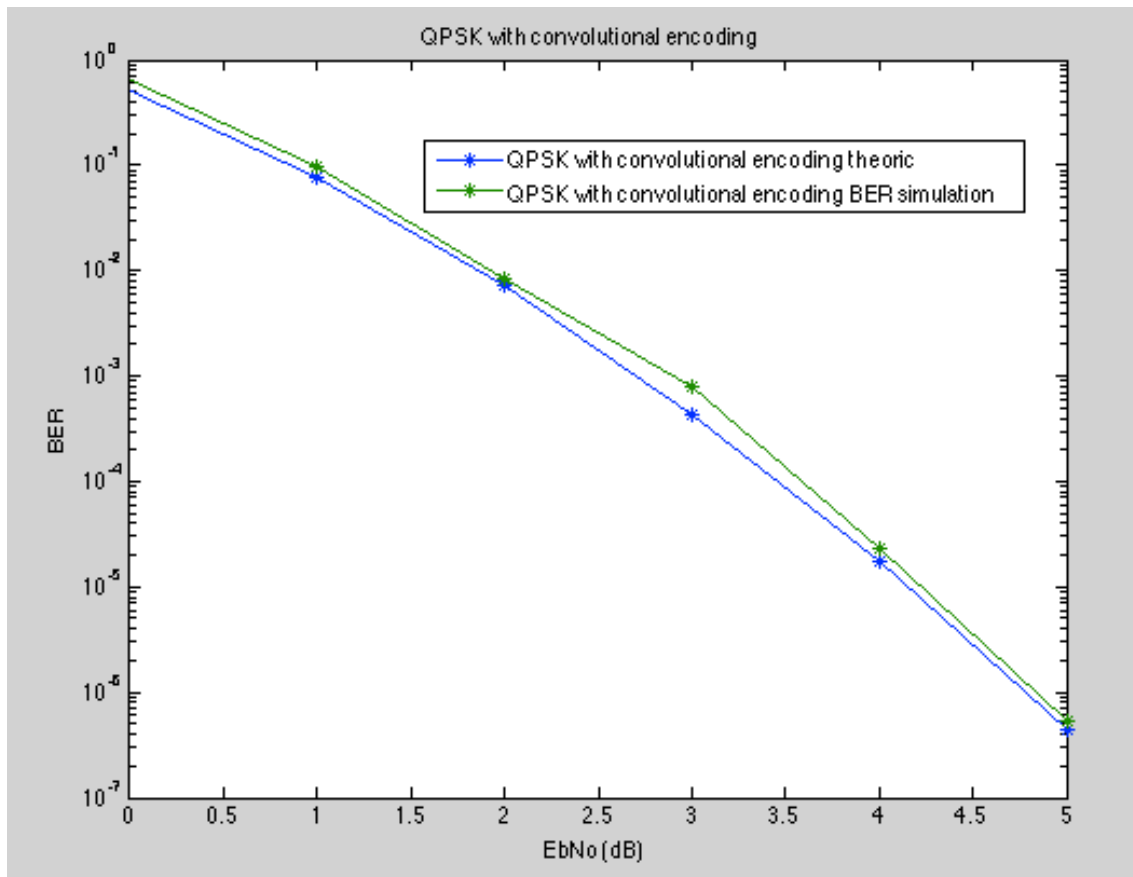


Figure 40: QPSK with Convolutional encoding BER comparative

As shown in the graphic of the Figure 40, the BER of the model simulated with Simulink, stands strong side by side with the theoretic line. In this case, the graphic ends up in $E_b/N_0=5$ dB because from 5 dB on, the model needs a computing model

too much large, because it need at least $2e^7$ sent bits, which requires so much time and processing capacity.

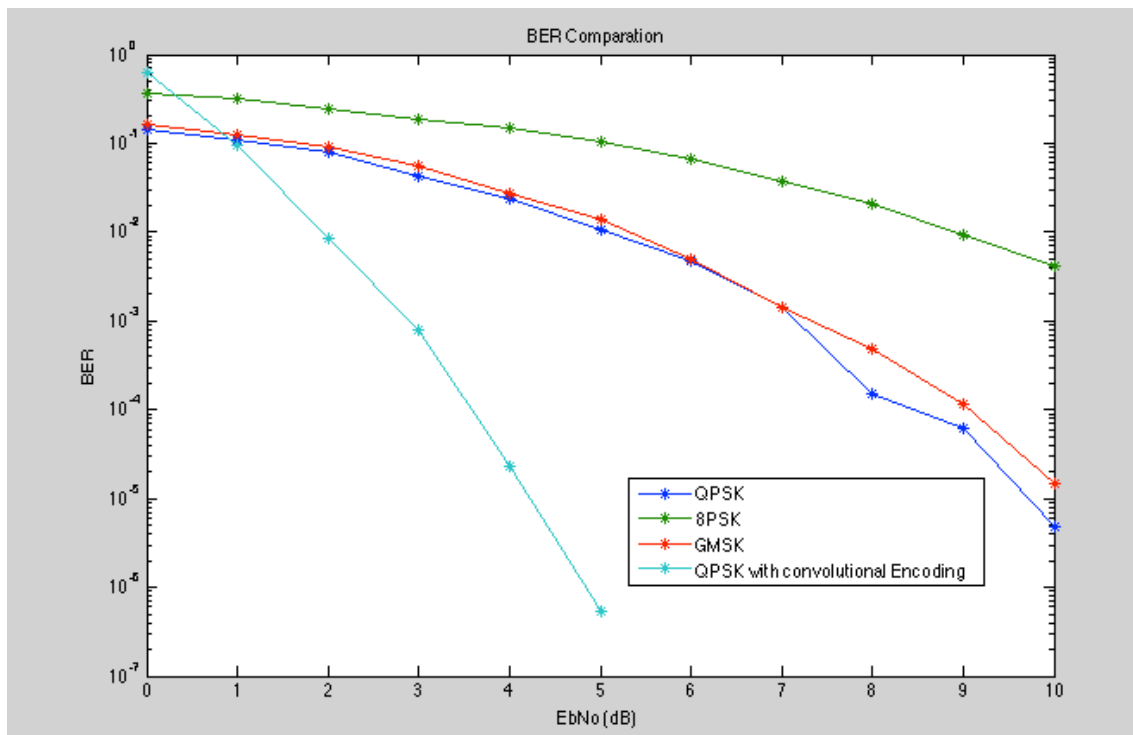


Figure 41: BER comparative between the 4 simulation

In the Figure 41 is shown the comparative between the 4 model simulations seen previously. As expected, the best simulation in terms of BER performance is the QPSK with Convolutional Encoding. The difference in terms of dB goes from 1 dB for low E_b/N_0 , to minimum 6 dB of difference in the $E_b/N_0=5$ dB.

5.2 Results discussion

Starting with the models without codification, the best performance is conducted by GMSK modulation. The Figure 35 shows that the calculated BER in the model matches almost perfectly with the theoretical curve. The case of QPSK and 8PSK, the BER performance is better in the case of QPSK. The explanation is simple: the QPSK is more robust against channel errors, because the information is concentrated in less bits. In the case of GMSK and QPSK, the BER performance is very close between them. It's a little better in the case of QPSK, but the difference is just about 0,5 dB. Clearly, the BER performance improves when we add codification to the system. It makes sense, since codification detects and in some of the cases corrects errors. The first samples have the same value, but when we add

more SNR, the results are very good with the codification, in front of the simulations without codification. So the final result it's the graphic shown in Figure 41, which demonstrates that QPSK with convolutional encoding improves the BER performance in an order of 1 to 7 dB.

CHAPTER 6

In this chapter a new communication subsystem applicable to the CONASAT project it's proposed. At the same time the preliminary calculation of the downlink it's done and several Simulink models for the modem link with their performance results are presented.

6.1 Communication Subsystem proposed

The communication service subsystem of satellites of the Conasat project are currently implemented with a transceiver board VHF / UHF Innovative Solutions in Space (ISIS) whose specifications are:

UHF Transmitter		VHF Receiver	
Frequency Range	400-450 MHz (Synthesized)	Frequency Range	130-170 MHz (Synthesized)
Transmit Power	500 mW Typical	Sensitivity	-100 dBm for BER 10e-5
Modulation	Raised - Cosine Binary Phase Shift Keying (BPSK)	Modulation	Audio Frequency Shift Keying, 1200 Hz/2200 Hz (Bell202)
Data Rate	1200, 2400, 4800, 9600 bit/s	Data Rate	1200 bit/s
Protocol	AX.25	Protocol	AX.25 command

Table 5: Current Conasat communication subsystem specifications

It should be noted, by specifying that the maximum bit rate downlink is 9600 B/s, a very low speed considering the current state of communication technologies. The proposal would use higher speed modems in order to have more flexibility for future generations of satellites of the Conasat project.

In the next section, the calculation of the link to determine the limit for the data rate transmission it's done.

6.2 Conclusions

All the models that were design in this project worked really well in the Matlab/Simulink simulations. Only in the case of the QPSK with convolutional encoding we had problems on the simulation. It was due to the computational time that was required to calculate the error rate for $E_b/N_0 > 5$ dB. But this only caused a longer time for computing the results. The major part of the errors that we faced

during the process were related with the sample times, and compilation errors due to the Matlab language.

The power efficiency in all cases was more than right, being in the worst case (GMSK) of 0.5 W, when the maximum calculated value was 0.75 W destined to communication in the Cubesat (explained in 3.2 Cubesat section of this project). So we're using in all cases less than the maximum 0.75 W of power calculated. All the measures in the simulations are done with a sample time 1e-7, which allows us to work in the S-BAND, and have a faster data rate to transmit the information.

In summary, in between the models simulated in this project, which matches most with the objectives that were proposed is the model with QPSK modulation and convolutional encoding. It has a really good BER performance, using the right frequencies and with a good bit rate. This may be the model used in a real SBCD transmission.

The communication system proposed for the near future includes a new modem transmitter, which would substitute the actual UHF Transmitter. The new transmitter would be a S-BAND modem, with a high speed modulation. After seeing the simulation results seen in chapter 5, it's been decided to use a QPSK modulation with convolutional codification. As explained in previous chapters, that change would not affect negatively to the power distribution of the Cubesat, and would significantly increase the data rate in the link. In the case of the QPSK, the data rate would be 2 times the actual data rate, just because the modulation is 2 times more frequency efficient than BPSK. To know the new data rate we are going to experiment with this new transmitter we are going to use the next information:

Distance satellite- Earth station= 600 Km;
 Frequency of the link = 2 GHz;
 Satellite's antenna's gain = 3 dB;
 Transmitter power = 0.5 W;
 Modulation = QPSK;
 Codification = convolutional;
 Earth station's antenna = 10 m diameter parabolic antenna;
 Earth station's receptor noise figure = 3 dB;
 Bit error rate = 10⁻⁵;
 Possible link's loss = 5 dB;

To calculate the gain of the parabolic Earth station's antenna G_t :

$$\lambda = \frac{c}{f} = \frac{3 \cdot 10^8}{2 \cdot 10^9} = 0.15 \text{ m}; \quad (6.1)$$

$$G_t = \frac{D^2}{\lambda^2} \eta = 2.222 \cdot 10^3; \quad (6.2)$$

where "D" is the diameter of the antenna (m), " λ " is the wavelength (m) and " η " is the antenna's efficiency, which is supposed to be 0.5. "c" is the light's speed (m/s) and f is the frequency of the link (Hz).

To calculate the received power in the Earth's antenna we use the following sentences:

$$P_r = P_t \left(\frac{\lambda}{4\pi d} \right)^2 \frac{G_t G_r}{L} = 0.5 \left(\frac{\lambda}{4\pi 600 \cdot 10^3} \right)^2 \frac{2.222 \cdot 10^3 \cdot 2}{3.1623} = 2.7810 \cdot 10^{-13} \text{ W}. \quad (6.3)$$

Where:

G_t = Gain of the transmitter's antenna;

G_r = Gain of the receptor's antenna;

d = Distance satellite- Earth station;

P_r = reception power;

P_t = transmit power;

L =Link's loss;

N_o is the noise density (W/Hz), k is the Boltzmann constant ($1,38 \cdot 10^{-23}$ W/Hz-K) and T_e is the noise temperature of the antenna.

$$T_e = (F-1)T_N = T_N = 290 \text{ k}, \quad (6.4)$$

where T_N is the equivalent temperature (k), and F is the Earth station's receptor noise figure.

$$N_o = kT_e = 1,38 \cdot 10^{-23} \cdot 290 = 4.0020 \cdot 10^{-21}. \quad (6.5)$$

In the Figure 40, it's shown that for a BER of 10^{-5} , it's necessary a E_b/N_o of 4.4 dB.

4.4 dB= 2.7542 linear.

$$\frac{E_b}{N_o} = 2.7542 \rightarrow E_b = 1.1022 \cdot 10^{-20}. \quad (6.6)$$

$$E_b = P_r / R_b, \quad (6.7)$$

where R_b is the data rate of the link.

$$R_b = \frac{P_r}{E_b} = 8.7944 \cdot 10^{-13} \frac{1}{1.1022 \cdot 10^{-20}} = 25.23 \text{ Mbps} \quad (6.8)$$

As expected, the data rate in this case is much faster with the QPSK modulation and the convolutional encoder, in this case, 25.23 Mbps.

S-BAND Transmitter		UHF Receiver	
Frequency Range	400-450 MHz	Frequency Range	130-170 MHz (Synthesized)
Transmit Power	0.5	Sensitivity	-100 dBm for BER 10e-5
Modulation	QPSK	Modulation	Audio Frequency Shift Keying, 1200 Hz/2200 Hz (Bell202)
Data Rate	25.23 Mbps	Data Rate	1200 bit/s
Protocol	AX.25	Protocol	AX.25 command
Codification	Convolutional	Frequency Range	130-170 MHz (Synthesized)

Table 6: Conasat communication subsystem proposed specifications

Other possibilities as the QPSK, GMSK or 8PSK simple models are also available, however they don't show so good results as the QPSK with convolutional codification model.

With QPSK model:

Distance satellite- Earth station= 600 Km;
 Frequency of the link = 2 GHz;
 Satellite's antenna's gain = 3 dB;
 Transmitter power = 0.5 W;
 Modulation = QPSK;
 Codification = none;
 Earth station's antenna = 10 m diameter parabolic antenna;
 Earth station's receptor noise figure = 3 dB;
 Bit error rate = 10⁻⁵;
 Possible link's loss = 5 dB;

To calculate the gain of the parabolic Earth station's antenna G_t :

$$\lambda = \frac{c}{f} = \frac{3 \cdot 10^8}{2 \cdot 10^9} = 0.15 \text{ m}; \quad (6.1)$$

$$G_t = \frac{D^2}{\lambda^2} \eta = 2.222 \cdot 10^3; \quad (6.2)$$

where "D" is the diameter of the antenna (m), " λ " is the wavelength (m) and " η " is the antenna's efficiency, which is supposed to be 0.5. "c" is the light's speed (m/s) and f is the frequency of the link (Hz).

To calculate the received power in the Earth's antenna we use the following sentences:

$$P_r = P_t \left(\frac{\lambda}{4\pi d} \right)^2 \frac{G_t G_r}{L} = 0.5 \left(\frac{\lambda}{4\pi 600 \cdot 10^3} \right)^2 \frac{2.222 \cdot 10^3 \cdot 2}{3.1623} = 8.7944 \cdot 10^{-13} \text{ W}. \quad (6.3)$$

Where:

G_t = Gain of the transmitter's antenna;

G_r = Gain of the receptor's antenna;

d = Distance satellite- Earth station;

P_r = reception power;

P_t = transmit power;

L =Link's loss;

N_o is the noise density (W/Hz), k is the Boltzmann constant ($1,38 \cdot 10^{-23}$ W/Hz-K) and T_e is the noise temperature of the antenna.

$$T_e = (F-1)T_N = T_N = 290 \text{ k}, \quad (6.4)$$

where T_N is the equivalent temperature (k), and F is the Earth station's receptor noise figure.

$$N_o = kT_e = 1,38 \cdot 10^{-23} \cdot 290 = 4.0020 \cdot 10^{-21}. \quad (6.5)$$

In the Figure 40, it's shown that for a BER of 10^{-5} , it's necessary a E_b/N_o of 9.7 dB, most of the twice of the QPSK with convolutional encoding.

4.4 dB= 9.3325 linear.

$$\frac{E_b}{N_o} = 9.3325 \rightarrow E_b = 3.7349e - 20. \quad (6.6)$$

$$E_b = P_r / R_b, \quad (6.7)$$

where R_b is the data rate of the link.

$$R_b = \frac{P_r}{E_b} = 8.7944 \cdot 10^{-13} \frac{1}{3.7349e^{-20}} = 23.54 \text{ Mbps} \quad (6.9)$$

As expected, the data rate is less than with the same modulation and the addition of a convolutional encoder. With 8PSK model the results are not satisfactory, because to reach a bit error rate of 10^{-5} a very high E_b/N_o is needed. With a GMSK modulation the results are the same as with the QPSK model.

6.3 Future perspectives

As future work, it would be interesting to prove the same models that were discussed here, but with a Reed-Solomon codification and another one with a concatenation of the convolutional and Reed-Solomon codes. These two have been very productive in satellite and spatial communications in the last 5 years.

In relation to the satellite network of the Brazilian government and its use and implementation, the CONASAT project proposes the constitution and development of a set (small constellation) of small satellites whose main mission is to collect environmental data, using orbits similar to the SCD-1 and SCD-2 whose coverages are adequate to Brazil. This project is going to be developed by the INPE (Instituto Nacional de Pesquisas Espaciais) and the AEB (Agencia Espacial Brasileira) in the near future.

In 2013 the SCD-1 completes 20 years in orbit, when its initial time of life was just 1 year.

References

- [1] Eduardo Escobar Bürger, *CUBESATS: MISSÃO INTEGRAÇÃO E TESTES, INSTITUTO NACIONAL DE PESQUISAS ESPACIAIS - INPE*, June 2012;
- [2] *Digital modulation techniques for mobile and personal communication systems - Electronics & Communication Engineering Journal*, November 2013;
- [3] *Introduction To Digital Modulation Schemes - The Design of Digital Cellular Handsets* (Ref. No. 1998/240), IEE Colloquium, November 2013;
- [4] California Politechnic State University, *Cubesat Requirements specifications*, November 2012;
- [5] *O SISTEMA BRASILEIRO DE COLETA DE DADOS AMBIENTAIS: ESTADO ATUAL, DEMANDAS E ESTUDOS DE PROPOSTAS DE CONTINUIDADE DA MISSÃO DE COLETA DE DADOS*, INPE, September 2013;
- [6] Sílvio A.Abrantes, *Simulação em Simulink da sincronização em comunicações digitais*, Universidade de Porto;
- [7] Sílvio A.Abrantes, *Introdução a sincronização em modulações digitais*, Universidade de Porto;
- [8] <http://www.mathworks.com/help/comm/examples/qpsk-transmitter-and-receiver.html>;
- [9] Thomas Wiegand and Heiko Schwarz, *Source Coding: Part I of Fundamentals of Source and Video Coding*, November 2010;
- [10] Fulvio Grassi Marangione, *Modelo Simulink para redes de comunicaciones ópticas multiservicio*, December 2007;
- [11] Hugo Andrés Angulo Orquera, *Diseño y desarrollo de un radio definido por software, mediante la utilización de una tarjeta USRP y la herramienta Simulink de Matlab*, 2011;
- [12] Luis Miguel Delgado Encinas, *Diseño e implementación de un módem con modulación QPSK*, Universidad de Valencia, September 2011;
- [13] Cory Edelman, *Presentation on Error Rate Simulation*, Agilent EEsof EDA;
- [14] Chris Noe, *Design and Implementation of the Communications Subsystem for the Cal Poly CP2 Cubesat Project*, June 2004;
- [15] http://www.teleco.com.br/Curso/Cbmod/pagina_3.asp, May 2014;
- [16] SCD information, http://www.inpe.br/scd1/site_scd/scd1/missao.htm, February 2014;
- [17] Convolutional coding, http://en.wikipedia.org/wiki/Convolutional_code;
- [18] Agencia Espacial Brasileira, <http://www.aeb.gov.br/>, May 2014;
- [19] Simulink and Matlab tutorials, <http://ctms.engin.umich.edu/CTMS/index.php?example=Introduction§ion=SimulinkControl#8>, May 2014;
- [20] <http://www.telecomabc.com/numbers/8psk.html>;
- [21] David Falconer, *Frequency Domain Equalization for Single-Carrier Broadband Wireless Systems*, April 2002;
- [22] <http://www.mathworks.com/help/dsp/ug/delay-and-latency.html#f12-98517>, April 2014;
- [23] http://www.itu.dk/stud/speciale/segmentering/Matlab6p5/help/toolbox/simulink/ug/how_simulink_works16.html, April 2014;
- [24] <http://edocs.soco.agilent.com/display/sv201103/Mapper>;
- [25] Joe Bauer, Michael Carter, Kaitlyn Kelley, Ernie Mello, Sam Neu, Alex

- Orphanos, Tim Shaffer, Andrew Withrow, *Mechanical, Power, and Thermal Subsystem Design for a CubeSat Mission*, April 2012;
- [26] University of Texas, *Communication's subsystem*, http://courses.ae.utexas.edu/ase463q/design_pages/spring03/cubesat/web/Paper%20Sections/4.0%20Communication%20Subsystem.pdf;
- [27] Adnane ADDAIM, Abdelhaq KHERRAS and El Bachir Zantou, *Design of Low-cost Telecommunications CubeSat-class Spacecraft*;